PERFORMANCE OF CONCRETE-FILLED DOUBLE-SKIN CIRCULAR TUBES IN COMPRESSION

By

YOOSUF ESSOPJEE

200709090

A Dissertation submitted to the Faculty of Engineering and the Built Environment as fulfilment of the requirements of the degree

MAGISTER INGENERIAE

in

CIVIL ENGINEERING SCIENCE

at the

UNIVERSITY OF JOHANNESBURG

SUPERVISOR: PROF. M DUNDU

MAY 2015

Abstract

CFDSCT columns are structural members that are filled with concrete and supported by circular steel tubes on the interior and exterior. These steel tubes serve as formwork and hence these members are economical and quicker to construct when compared to conventional concrete reinforced columns. They are also efficient because they take advantage of the high compressive strength of the concrete and high tensile strength of steel. Despite the fact that much research is ongoing internationally in the field of CFDSCTs, no experimental tests have been conducted on intermediate and slender CFDSCTs. Current research has been focused on short CFDSCT columns and varying amounts of confinement have been found in these tests. Design codes also do not cover CFDSCTs. In order to gain a more comprehensive understanding of the behaviour of CFSDSCTs, experimental tests were conducted on 32 concrete-filled double-skin circular tube (CFDSCT) columns. The CFDSCT columns were loaded in axial compression till failure. The parameters that were varied were the lengths and diameters of the outer steel tubes, and the strength of the outer steel tubes. The lengths ranged from 1 and 2.5 m, in half a metre increments. The CFDSCTs of one metre lengths, failed by yielding of the steel tubes. All the other CFDSCTs failed by overall buckling due to their large slenderness. Using the same philosophy as SANS 10162-1 and EC4, new formulas were developed to predict the results of the strengths of the CFDSCTs. The new formulas are in a similar format to SANS 10162-1 and EC4, and are 5% and 6% more conservative than the tests results, respectively. The ratio of the predicted results over the test results versus the slenderness was plotted and shows that the results were predicted fairly well.

Acknowledgments

It is only through the grace and great favours of Allah (SWT) upon me that I have been able to do this research.

"He who is not grateful to mankind cannot be grateful to Allah." Tirmidhi

I would like to thank the following people:

My father, for his continuous encouragement. It is because of his counsel that I enrolled for the master's degree.

My mother, wife, sisters and other family members for their continuous support. I would never be able to repay your favours upon me.

I am very grateful to Prof. Dundu for his continuous support, encouragement and patience. He has been much more than a study leader to me.

All the university staff who had assisted me with the laboratory work.

Pronto Ready-mix for generously sponsoring the concrete.

Transnet for encouraging and supporting their staff to pursue higher education.

TABLE OF CONTENTS

LIST OF FIGURES

LIST OF TABLES

LIST OF SYMBOLS

D_o	Outer tube diameter
D_i	Inner tube diameter
t_o	Thickness outer tube
t_i	Thickness inner tube
f_{yi}	Yield strength of inner tube
f_{yo}	Yield strength of outer tube
N_T	Experimental compressive strength
N_P	Predicted compressive strength
B_o	Breadth of outer tube
B_i	Breadth of inner tube
N_u	Ultimate strength
A_{so}	Area of steel outer tube
A_{si}	Area of steel inner tube
A_c	Area of concrete
f_c'	Compressive strength of concrete
E_s	Modulus of elasticity
f_y	Yield strength of steel
f_u	Ultimate strength of steel
g	Grams
kN	Kilo Newton
MPa	Megapascals
GPa	Gigapascals
λ	Relative slenderness
E_{si}	Young's modulus for inner steel tube
I_{si}	Moment of inertia for inner steel tube
E_{so}	Young's modulus for outer steel tube
I_{so}	Moment of inertia for outer steel tube
E_c	Young's modulus for concrete
I_c	Moment of inertia for concrete
K	Effective length factor

L	Length of column
τ	Steel reduction factor
τ'	Concrete enhancement factor
C_{ec}	Euler buckling strength
EI_e	Elastic flexural stiffness
X	Reduction factor

LIST OF ABBREVIATIONS

ACI	American concrete institute
CFCT	Concrete-filled circular tube
CFDSCT	Concrete-filled double-skin circular tube
CFDSRT	Concrete-filled double-skin rectangular tube
CFDSSCT	Concrete-filled double-skin square-circular tube
CFT	Concrete-filled tube
CHS	Circular hollow section
EC	Euro code
FEA	Finite element analysis
FEM	Finite element model
LCD	Liquid crystal display
SANS	South African national standards

1. Introduction

Concrete-filled steel tubes (CFST) are valuable structural members that are filled with concrete and supported on the exterior by steel tubes. CFST can be constructed in various shapes and examples of square and circular CFST are shown Figure 1. These members are economical and quicker to construct, compared to conventional concrete-reinforced columns.

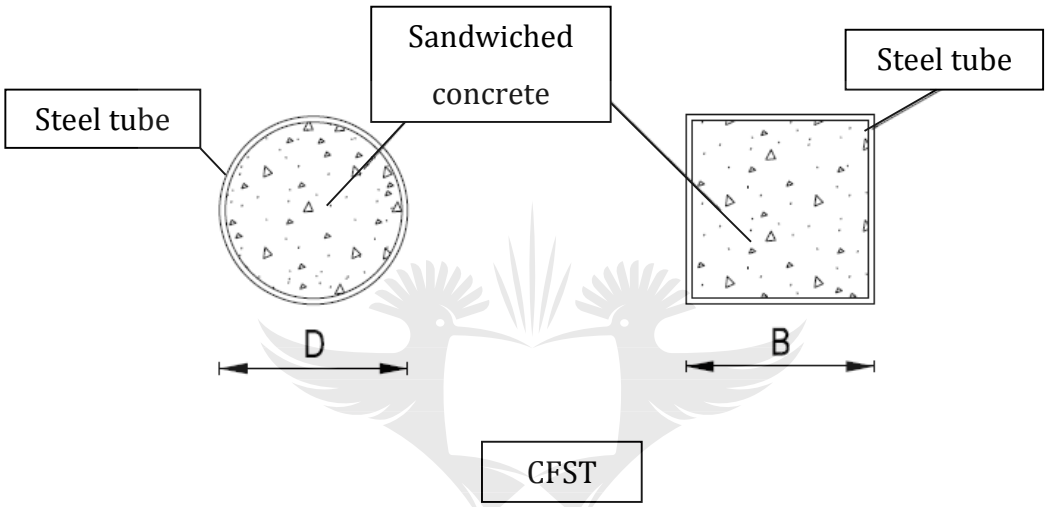

Figure 1 : CFST columns

In multi-storey buildings architects may detail downpipes or other services such as electrical wiring in the centre of columns. This is done for aesthetic reasons. One way of achieving this is to use concrete-filled double-skin tubes (CFDSTs). Concrete-filled double-skin tubes (CFDSTs) are structural members that have a double steel skin with concrete sandwiched between the two steel tubes. These structural elements can be concrete-filled double-skin rectangular tubes (CFDSRTs), concrete-filled double-skin circular tubes (CFDSCTs) or concrete-filled double-skin rectangular-circular tubes (CFDSRCTs), as shown in Figure 1.

Just like CFTs, these members are also economical and quicker to construct than conventional concrete-reinforced columns because the steel tube serves as form-work. This means that high rise buildings can be completed swiftly when CFDST columns are used. The concrete fill prevents the outer steel tube from buckling inwards whilst the steel prevents the concrete from deforming laterally, under compressive loads. CFDST

columns have structural benefits similar to concrete-filled tube (CFT) columns. In addition they are lighter, stronger and possess better energy absorption (Elchalakani, 2002; Zhao, 2002)

When CFDST columns were subjected to cyclic loading and axial loading, Yagishita (2000) found that they had higher ductility, energy absorption and strength. Similar conclusions were also reached by Nakanishi (1999), who tested CFDSTs and CFTs cyclically. Hence, CFDSTs have an important role in earthquake-affected countries.

CFDSTs have better fire resistance than CFTs and empty tubes (Li, 2012). Li (2012) also found that there was composite action between the concrete and steel during exposure to fire and this is favourable in terms of fire performance.

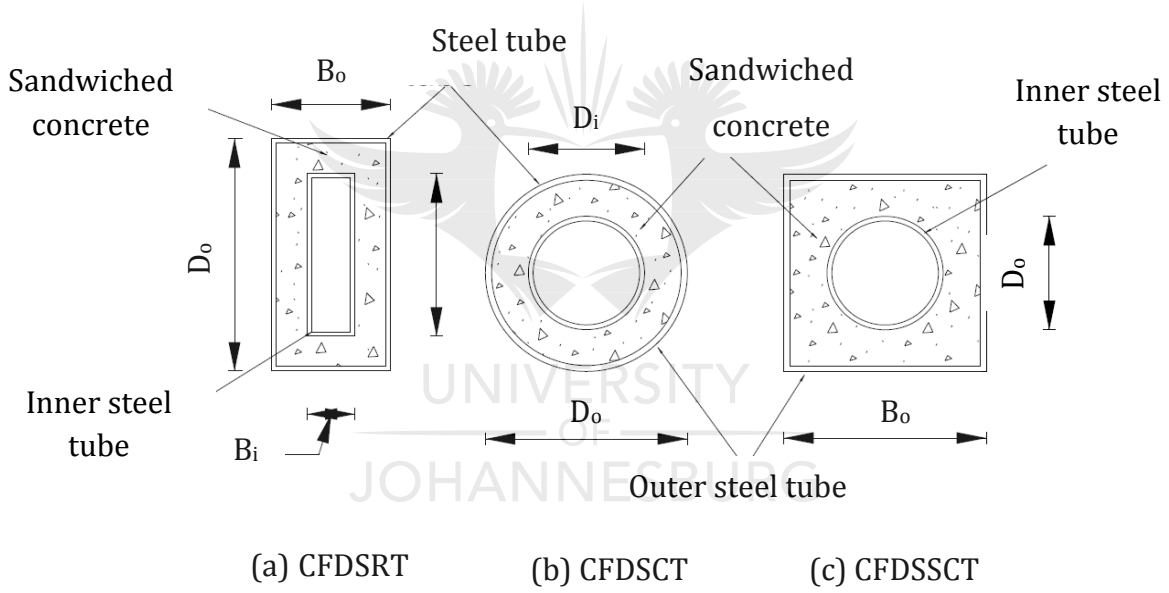

Figure 2: Different shapes for CFDSTs

Despite the fact that much research is ongoing internationally in the field of CFDSCTs, no experimental tests have been conducted on intermediate and slender CFDSCTs. Current research has been based on short CFDSCT columns which are intended to give guidance on the design of slender CFDSTs. Various authors have also found different amounts of confinement in their tests.

Design codes also do not cover CFDSCTs. They however cover CFTs which are similar but behave differently. To better understand the behaviour of CFSDSCTs, it is proposed that research is conducted on intermediate and slender CFDSCT columns. The results found from the tests will be used to formulate proposals for implementation in SANS 10162-1 and EC4.

2. Literature review

2.1 Introduction

The purpose of this literature review is to summarise all the relevant research that has been conducted on concrete-filled double-skin circular tubes (CFDSCTs).

Concrete-filled double-skin tubes (CFDSTs) are a recent development, with most research occurring in the last two decades. Most of the research on CFDSCT columns has been conducted in China. Research has also been conducted in Australia, Egypt, Japan, Singapore and the United States of America.

Zhao and Han (2006) have conducted a review of the work on CFDSCTs. They have summarized this research in their paper titled “Double skin composite construction”.

Different cross-sections of CFDST columns have also been investigated by other researchers. Elchalakani et al. (2002) have done research on CFDSTs that have a square hollow section (SHS) inner and CHS outer tubes. All the columns tested were stub columns, with slenderness ratios ranging from 35 and 90. It was found that the strength of the individual components predicted the test results well.

Yang et al. (2008) conducted research on an octagonal outer tube and a circular inner tube. From this experiment, it was found that the axial capacity of the proposed CFDST was larger than that of a square section outer tube and smaller than that of a circular section outer tube. The CFDSTs were modelled numerically. A simplified formula was suggested and the numerical results simulated the proposed results reasonably well.

In this literature review, the aim of each investigation, the parameters of the tests, the modes of failure and the results are stated and discussed. Formulae proposed by the authors are also discussed.

2.2 Wei et al. (1995)

The aim of this research was to test the compressive strength of the CFDSCT columns with polymer concrete sandwiched between two steel tubes. A total of 26 samples were tested. The diameters of the outer tubes ranged from 74.7 to 114.3 mm. The inner tube diameters ranged from 61.2 to 88.9 mm. The diameter-to-thickness ratio of the outer tubes varied from 43 to 169. The range is broad and represents what would be used in engineering practice. Aggregates made up 86 % of the polymer concrete in terms of its weight and the remaining 14 % was polymer resin. The polymer concrete strength was 75 MPa. As shown in Table 1, the yield strengths of the inner tubes and outer tubes ranged from 216 to 512 MPa and 255 to 524 MPa respectively. All the stub columns were machined to a length of 230 mm.

The end conditions were simulated as pinned and an axial load was applied using a Tinius Olesen machine. The specimens failed by local buckling of the outer tube. The inner tubes also buckled locally at the middle of the columns. Specimens were cut open and it was also found that the concrete had failed by shear in the buckled region.

In Table 1, N_T represents the experimental compressive strength and N_P represents the sum of the strengths of the individual components (two tubes plus the concrete infill). It can be seen from this table that all the test results are greater than the predicted results. The average test strength of the CFDSCT is 15% larger than the sum of the strengths of the individual components, with test strengths up to 31% larger than the predicted strengths. The test-to-predicted strength in Table 1 suggests that the test values can conservatively be represented by the sum of the individual strengths of the materials. The difference between the experimental and predicted strengths is due to concrete confinement between the steel tubes.

Table 1 : Wei et al. test results

Test	D_o (mm)	D_i (mm)	$\frac{D_o}{t}$	$\frac{D_i}{t}$	f_{yi} (MPa)	f_{yo} (MPa)	N_T (kN)	N_P (kN)	$\frac{N_T}{N_P}$
1	74.8	62	73	62	470	486	283	264	1.07
2	74.7	62	77	66	470	486	285	254	1.12
3	75.4	62.7	58	51	470	486	348	325	1.07
4	75.2	62.4	63	52	470	486	348	314	1.11
5	76.3	62	43	62	470	486	395	350	1.13
6	76.3	62	44	66	470	512	395	353	1.12
7	81	62	90	62	470	524	330	303	1.09
8	81	62	93	66	470	524	335	294	1.14
9	81.5	62.7	73	55	470	524	386	348	1.11
10	81.5	62.2	71	55	470	524	395	350	1.13
11	87.4	61.8	88	71	452	428	378	338	1.12
12	87.3	61.6	93	70	452	428	385	332	1.16
13	87.9	61.4	70	69	452	428	432	363	1.19
14	87.9	61.2	75	72	452	444	408	371	1.1
15	99.7	80.3	169	146	474	409	283	238	1.19
16	99.9	86.8	145	142	444	409	299	228	1.31
17	99.9	80.5	141	120	474	409	357	275	1.3
18	99.9	74	143	119	512	409	380	302	1.26
19	99.8	61.4	151	112	432	409	443	389	1.14
20	101.7	61.5	63	110	432	409	644	541	1.19
21	88.8	63.5	57	55	216	286	357	319	1.12
22	101.4	63.4	65	55	216	255	477	426	1.12
23	101.5	76.1	62	64	235	255	417	363	1.15
24	114.3	63.5	70	57	216	262	598	549	1.09
25	114.3	76.1	70	67	235	262	551	492	1.12
26	114.3	88.9	70	57	286	262	524	460	1.14

2.3 Tao et al. (2003)

Tao et al. (2003) conducted research into the behaviour of CFDSCT stub columns and beam columns. Note that only the stub columns will be discussed as the beam columns fall outside the scope of this research. They conducted 12 tests on CFDSCT stub columns. The lengths of the stub columns varied from 342 to 900 mm. Two concrete-filled circular tube (CFCT) columns were also tested in order to compare the results against the CFDSCT results. The concrete cube strength was 47 MPa at the time of the test and the yield strength of the steel inner tube (f_{yi}) ranged varied from 295 to 396 MPa, while that of the outer tube (f_{yo}) was either 276 or 295 MPa. It can be seen that the outer steel tube has a low strength and the concrete has a high strength. The concrete strength is higher than what would normally be used in engineering practice. As given in Table 2, the outside tube diameters (D_o) were 114, 180, 240 and 300mm and the inside tube diameters (D_i) were 48, 58, 88, 114, 140 and 165 mm. The end conditions were simulated as pinned and axial load was applied.

The failure mechanism of the outer tubes was local buckling. As for the inner tubes, those with larger diameter-to-thickness ratios failed by inward local buckling of the tube, whilst the tubes with smaller diameter-to-thickness ratios showed no sign of buckling. In Table 2, N_T represents the experimental compressive strength and N_P represents the sum of the strengths of the individual components (two tube/s plus the concrete infill).

Table 2 : Tao et al. test results

Test	D_o (mm)	D_i (mm)	$\frac{D_o}{t_o}$	$\frac{D_i}{t_i}$	f_{yi} (MPa)	f_{yo} (MPa)	N_T (kN)	N_P (kN)	$\frac{N_T}{N_P}$
1	180	-	60	-	-	276	1680	1547	1.09
2	180	-	60	-	-	276	1618	1547	1.05
3	180	48	60	16	396	276	1790	1633	1.1
4	180	48	60	16	396	276	1791	1633	1.1
5	180	88	60	29	370	276	1648	1566	1.05
6	180	88	60	29	370	276	1650	1566	1.05
7	180	140	60	47	342	276	1435	1285	1.12
8	180	140	60	47	342	276	1358	1285	1.06
9	114	58	38	19	375	295	904	830	1.09
10	114	58	38	19	375	295	898	830	1.08
11	240	114	80	38	295	276	2421	2376	1.02
12	240	114	80	38	295	276	2460	2376	1.04
13	300	165	100	55	321	276	3331	3283	1.01
14	300	165	100	55	321	276	3266	3283	0.99

With the exception of one result, all test results were greater than the predicted results. The average strength difference between the test and predicted results was 6%, with a maximum difference of 10%.

Based on the results in Table 2, it is suggested that no concrete confinement exists in CFDSCTs. A basic formula was proposed to define the strengths of these stub columns (Equation 1).

$$N_u = \left(C_1 \chi^2 f_{syo} + C_2 (1.14 + 1.02\xi) f_{ck}\right) A_{sco} + A_{si} f_{syi} \quad (1)$$

Where, χ is the hollowness ratio of the inner tube over the outer tube, ξ is the confinement factor that is equal to the product of the area of steel and yield stress of steel divided by the product of the area of concrete and the yield stress of the concrete, f_{syo} is the yield strength for the outer tube, f_{ck} is the cylindrical strength for the concrete, A_{sco} is the area of the outer tube and sandwiched concrete, A_{si} is the area of the inner steel tube and f_{syi} is the yield strength of the inner tube, $C_1 = \alpha/(1+\alpha)$ and $C_2 = (1+\alpha)/(1+\alpha_n)$. In C_1 and C_2, α is equal to the area of steel over the area of concrete and α_n is the same with only the nominal area of concrete. Equation 1 is a modification of the sum of the individual strengths of the steel tubes and concrete. Tao et al. (2003) also proposed that the inner

steel tube only acts compositely when the hollowness ratio is less than 0.8. It is clear from the results in Table 2 that although Equation 1 suggests that the outer tube causes enhancement, there is little or no enhancement in the experimental results.

2.4 Zhao et al. (2002)

Zhao et al. (2002) carried out tests to assess the behaviour of six CFDSCT stub columns. The length of all the stub columns was 400 mm. The concrete strength was 78.4 MPa at 28 days and the yield strength of the steel inner tube (f_{yi}) and outer tubes (f_{yo}) varied from 395 to 454 MPa. The strength of the concrete is high and would not normally be used in engineering practice. The concrete strength is also higher than in all the other research reviewed. The diameter of the external tubes (D_o) was 114 or 165 mm and that of the inside tubes (D_i) was either 48 or 102 mm. The diameter-to-thickness ratios of the outer and inner tubes ranged from 19 to 57 and 17 to 33 respectively. An axial load was applied and the end conditions were pinned. Tests were also conducted on the inner and outer steel tubes individually without concrete fill. The results from the steel tubes tests are summarised in Table 3.

Table 3 : Zhao et al. steel tubes

Test	Location	Diameter	N_T(kN)
1	Outer	114.5	927
2	Outer	114.6	719
3	Outer	114.4	560
4	Outer	114.2	454
5	Outer	165.1	674
6	Outer	165.3	553
7	Inner	48.4	228
8	Inner	101.8	414

The experimental results from the empty steel tubes were relatively close to the predicted strength based on the material yield values, with a mean value of four percent. Tests were then conducted on the CFDSCT stub columns. The results are presented in Table 4.

The outer tubes failed by local outward buckling. These were categorised by outward folding near the bottom ends and diagonal failure near the centre. The inner tubes failed by inward local buckling. This is consistent with the mode of failure found by Tao et al. (2003) and Wei et al. (1995).

Table 4 : Zhao et al. CFDSCT test results

Test	D_o (mm)	D_i (mm)	$\frac{D_o}{t_o}$	$\frac{D_i}{t_i}$	f_{yi} (MPa)	f_{yo} (MPa)	N_T (kN)	N_P (kN)	$\frac{N_T}{N_P}$
1	114.5	48.4	19	17	425	454	1415	1432	0.99
2	114.6	48.4	24	17	425	416	1380	1215	1.14
3	114.4	48.4	33	17	425	453	1210	1112	1.09
4	114.2	48.4	38	17	425	430	1110	1017	1.09
5	165.1	101.8	47	33	410	433	1705	1783	0.96
6	165.3	101.8	57	33	410	395	1605	1617	0.99

The average test results are 4% higher than the predicted results. However, the ratio of the test strengths to the predicted strengths lies between 0.96 and 1.14. Based on these results, it is clear that there is no confinement in these stub columns.

2.5 Uenaka et al. (2009)

The aim of this research was to test CFDSCT stub columns loaded axially and to derive an equation to predict their strengths. This research tested 12 stub columns in total. Nine out of the twelve samples were CFDSCT stub columns and the remainder were CFT columns. The concrete strength was 23 MPa. Outer tubes had an average dimension of 158 mm while the average dimensions of the inner tubes were 39, 77 and 114mm. The inner and outer steel tubes' strengths ranged from 221 to 308 MPa and each stub column was 450 mm in length.

The columns were subjected to axial load under pinned conditions. Both the inner and the outer tubes failed as a result of local buckling. The inner tubes failed by inward buckling whilst the outer tubes failed by outward buckling. The concrete infill failed by shear. In Table 5, N_T represents the experimental compressive strength and N_P represents the sum of the strengths of the individual components (tube/s plus the concrete infill).

Table 5 : Uenaka et al. CFDSCTs test results

Test	D_o (mm)	D_i (mm)	$\frac{D_o}{t_o}$	$\frac{D_i}{t_i}$	f_{yi} (MPa)	f_{yo} (MPa)	N_T (kN)	N_P (kN)	$\frac{N_T}{N_P}$
1	159	-	176	-	221	221	700	497	1.41
2	158	38	176	43	221	221	635	450	1.41
3	159	76	176	84	221	221	540	440	1.23
4	159	114	176	126	221	221	378	395	0.96
5	158	-	105	-	308	308	815	581	1.4
6	158	39	105	26	308	308	852	648	1.31
7	158	77	106	51	308	308	728	640	1.14
8	158	114	106	76	308	308	589	542	1.09
9	158	-	74	-	286	286	908	680	1.33
10	158	40	74	19	286	286	968	705	1.37
11	158	77	74	36	286	286	879	752	1.17
12	157	115	73	54	286	286	704	697	1.01

Uenaka et al's test-to-predicted strengths, given in Table 5, imply that there is significant concrete confinement in the CFDSCT and that the concrete confinement exists only because of the outer tube. Accordingly the effect of confinement became smaller as the internal diameter increased. The strength enhancement ranges from almost 0 to 41%, and based on these experimental results Equation 2 was developed.

$$N_u = [2.86 - 2.59(d_i / d_o)]A_{so} f_{yo} + A_{si} f_{yi} + A_c f_c^{'} \quad (2)$$

$$0.2 \leq di/do \leq 0.7$$

where, N_u is the axial capacity, D_i is the inner tube diameter, D_o is the outer tube diameter, A_{so} is the area of the outer tube, f_{yo} is the yield strength of the outer tube, A_{si} is the area of the inner tubes, f_{yi} is the yield strength of the inner tube, A_c is the area of concrete and f'_c is the cube strength of the concrete. Similarly to Equation 1, Equation 2 is a modification of the sum of the individual strengths of each material. As indicated above, the results obtained vary by a large margin. Such a large variation casts doubt on the accuracy of Equation 2.

2.6 Wei et al. (2012)

Wei et al. (2012) conducted research into the behaviour of CFDSCT stub columns that were tapered. A total of 12 samples were tested in axial compression. The heights of the stub columns ranged from 750mm to 1050mm. Of the 12 samples tested, 2 were not tapered and had the same diameter at each end. Self-compacting concrete, with strength of 50 MPa at 28 days, was used, and the strength was 52.5 MPa at the time of testing. The outer steel tube was 3.82 mm thick while the inner tube was 2.92mm thick. The yield strength of the inner and outer tubes was 397 and 509 MPa respectively. A schematic illustration of the samples is shown in Figure 3. The dimensional properties are given in Table 6. In Table 6, N_T represents the experimental compressive strength and N_P represents the predicted strength calculated from the formula proposed by Tao et al. (2003) sum of the strengths of the individual components (two tapered tubes plus the concrete infill).

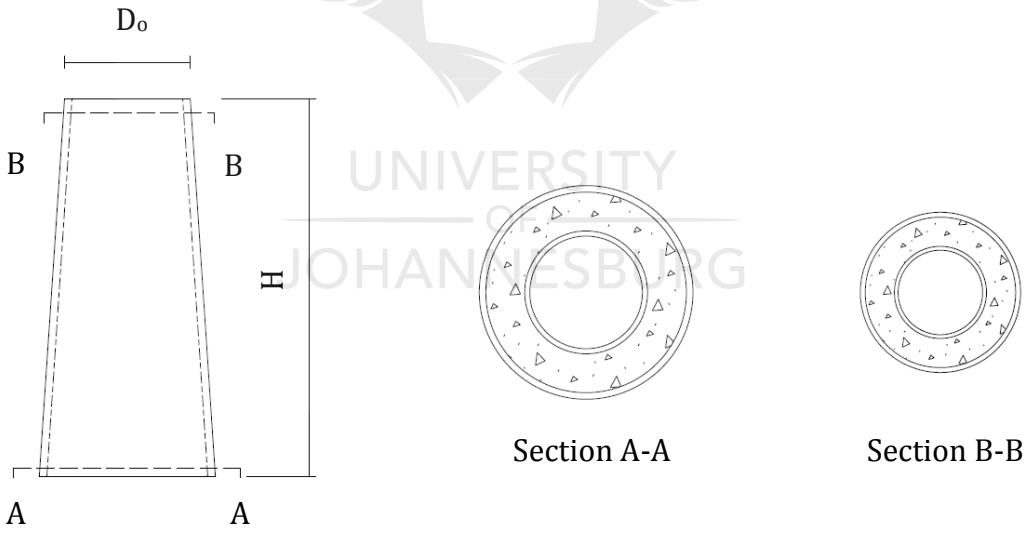

Figure 3 : Tapered columns

Table 6 : Tapered stub columns dimensional properties and strengths

Test	Outer tube		Inner tube		Height mm	angle Θ	N_T (kN)	N_P (kN)	$\frac{N_T}{N_P}$
	A-A (mm)	B-B (mm)	A-A (mm)	B-B (mm)					
1	350	350	231	231	1050	0	5499	5448	1.01
2	350	350	231	231	1050	0	5396	5448	0.99
3	329	350	210	231	1050	0.57	4942	4932	1.00
4	329	350	210	231	1050	0.57	4921	4932	1.00
5	308	350	189	231	1050	1.14	4569	4585	1.00
6	308	350	189	231	1050	1.14	4600	4585	1.00
7	282	300	180	198	900	0.57	3874	3961	0.98
8	282	300	180	198	900	0.57	4048	3961	1.02
9	235	250	150	165	750	0.57	3090	3103	1.00
10	235	250	150	165	750	0.57	3116	3103	1.00
11	329	350	210	231	1050	0.57	2163	2198	0.98
12	329	350	210	231	1050	0.57	2233	2198	1.02

The columns were subjected to axial load under pinned conditions.

Figure 4 shows that the failure mechanism of the outer tubes was local outward buckling. However, the inner tubes buckled inwardly combined with the crushing of the concrete.

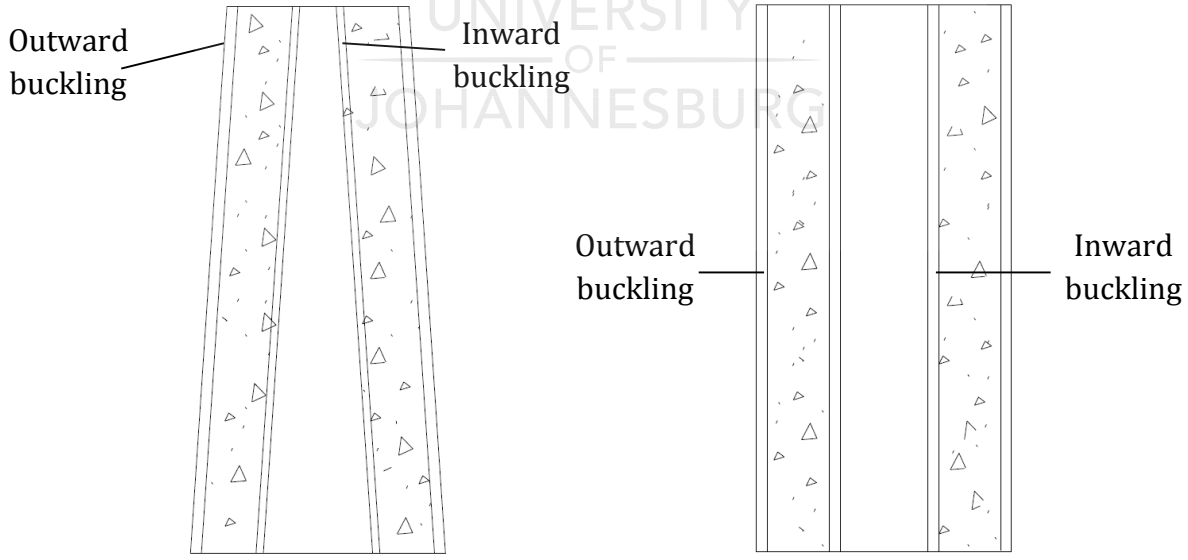

Figure 4 : Mode of failure

The predicted strength was calculated from the formula proposed by Tao et al. (2003). The formula is the same formula reviewed in section 1.2. Hence, the research suggests that the strength of short tapered sections can be determined by finding the strength of the smallest cross sectional area. Hence, the cross-sectional areas used in the calculation for the different materials are the minimum values. It can be seen from the ratios that the predicted strength are almost the same as the experimental strength. Hence, the formula proposed by Tao et al. (2003) is valid for tapered CFDSCT stub columns.

2.7 Tan and Zhang (2010)

Tan and Zhang (2010) conducted research into a proposal for a formula for CFSCTs. Their formula was based on the experimental tests conducted by others. The capacities of 15 axially loaded CFDSCT stub columns were studied.

The experimental samples discussed in this paper were those tested by Wei et al. (1995) and Tao et al. (2004) described in Sections 2.2 and 2.3, respectively. Hence, the material properties for these CFDSCTs can be found in those sections.

The formula below is for the equivalent confinement coefficient:

$$\tau' = \frac{\sum As.fs}{Ac.fc} = \frac{A_{so} \times f_{so} + A_{si} \times f_{si}}{A_c \times f_{cu}} \quad (3)$$

The authors have labelled τ' the confinement coefficient. This implies that the concrete core confinement is derived from both the inner and outer steel tubes.

$$fssc = (1.212 + a.\tau_{scc} + b.\tau_{ssc}^2)fcu \quad (4)$$

Where:

$$a = \frac{0.1759fss}{235} + 0.974 \quad (5)$$

$$b = \frac{-0.1038fck}{20} + 0.309 \quad (6)$$

$$fss = \frac{Aso.fso + Asi.fsi}{Aso + Asi} \quad (7)$$

Hence, a new design methodology for CFDSCTs is proposed. The nature of the numerical values in the formulas above show that these formulas are based on a best fit curve. The new proposed formulas are evaluated against the tests results from Wei et al. (1995) and Tao et al. (2004) and are shown in Table 7 and 8 respectively. N_T represents the experimental compressive strength and N_P represents the sum of the strengths of the individual components (two tubes plus the concrete infill).

Table 7 : Tan and Zhang test results

Test No	D_o (mm)	D_i (mm)	$\frac{D_o}{t_o}$	$\frac{D_i}{t_i}$	f_{yi} (MPa)	f_{yo} (MPa)	$\frac{A_s}{A_c}$	N_T (kN)	N_p (kN)	$\frac{N_T}{N_P}$
1	74.8	62	73	62	470	486	0.318	283	240	1.18
2	75.4	62.7	58	51	470	486	0.401	348	234	1.48
3	81	62	90	62	470	524	0.199	330	336	0.98
4	87.4	61.8	88	71	452	428	0.147	378	380	0.99
5	99.9	74	143	119	512	409	0.102	380	392	0.97
6	99.8	61.4	151	112	432	409	0.064	443	429	1.03
7	114.3	63.5	70	57	216	262	0.115	598	619	0.96
8	114.3	76.1	70	67	235	262	0.151	551	557	0.99
9	114.3	88.9	70	57	286	262	0.252	524	515	1.02

Table 8 : Tan and Zhang test results

Test No	D_o (mm)	D_i (mm)	$\frac{D_o}{t_o}$	$\frac{D_i}{t_i}$	f_{yi} (MPa)	f_{yo} (MPa)	$\frac{A_s}{A_c}$	N_T (kN)	N_p (kN)	$\frac{N_T}{N_P}$
10	180	48	60	16	396	276	0.091	1790	1762	1.02
11	180	88	60	29	370	276	0.13	1649	1712	0.96
12	180	140	60	47	342	276	0.3	1396	1331	1.05
13	114	58	38	19	375	295	0.214	901	863	1.04
14	240	114	80	38	295	276	0.095	2440	2610	0.93
15	300	165	100	55	321	276	0.089	3298	3642	0.91

It is shown that the predicted strengths are in an acceptable range when compared to the experimental strengths, except when the steel-to-concrete area ratio is large (greater than 0.3).

2.8 Hassanein et al. (2013a)

Hassanein et al. (2013a) performed a finite element analysis of the work conducted by Tao et al. (2003). The CFDSCTs tested by Tao et al. (2004) were modelled in ABAQUS. Only a quarter of the CFDSCT was modelled. Cover plates were modelled at both ends to simulate uniform load distribution on the material surfaces. Load was applied to the top cover plate. The bottom end was fixed and the top end was allowed to move in the direction of the load. The friction coefficient was set to 0.4 between the concrete and steel tube. The results from the FE analysis are shown in Table 9. In Table 9, N_{FE} represents the axial strength found by Finite Element analysis, N_{EXP1} and N_{EXP1} represent the experimental strength of the CFDSCTs found by Tao et al. (2004).

Table 9 : Comparison of FE results with test results by others

Column	D_o (mm)	D_i (mm)	$\frac{D_o}{t_o}$	$\frac{D_i}{t_i}$	L (mm)	f_{yo} (MPa)	f_{yi} (MPa)	$\frac{N_{FE}}{N_{EXP1}}$	$\frac{N_{FE}}{N_{EXP2}}$
1	180	48	60	16	540	276	396	0.97	0.96
2	180	88	60	29	540	276	370	0.95	0.95
3	180	140	60	47	540	276	342	1.00	0.94
4	114	58	38	19	342	295	375	1.00	1.01
5	240	114	80	38	720	276	295	0.99	0.97
6	300	165	100	55	900	276	321	0.98	1.00

The FE model was used to predict the strength of CFDSCTs with carbon steel inner and outer tubes, as tested by Tao et al. (2004) and of CFDSCTs with stainless steel outer tubes and carbon steel inner tubes, as tested by Han et al. (2011).

Since Han et al. (2011) did not give full details on the types of stainless steel, Hassanein et al. (2013a) modelled the tubes to have carbon steel outer and inner tubes. They then modelled 48 samples with stainless steel outer and carbon steel inner tubes and discussed their results. The content of this is not covered in this review since stainless steel falls outside the scope of this research.

Equations 8, 9 and 10 were proposed for stainless steel outer and carbon steel inner tube CFDSCT stub columns:

$$N_U = \alpha_{so}\sigma_{0.2}A_{so} + \alpha_{si}f_{yi}A_{si} + (\alpha_c f_c + 4.1f_{so})A_c \quad (8)$$

$$\alpha_{so} = 1.62\left(\frac{D_o}{t_o}\right)^{-0.1} \quad (9)$$

$$\alpha_{si} = 1.458\left(\frac{D_i}{t_i}\right)^{-0.1} \quad (10)$$

Where $\alpha_{so} \leq 1.2$ and $0.9 \leq \alpha_{si} \leq 1.1$

In Equations 8 - 10, N_u is the axial capacity, D_i is the inner tube diameter, D_o is the outer tube diameter, A_{so} is the area of the outer tube, f_{so} is the strength of the outer tube, A_{si} is the area of the inner tubes, f_{yi} is the yield strength of the inner tube, A_c is the area of concrete and f_c is the cylindrical strength of the concrete. $\sigma_{0.2}$ is the proof stress for stainless steel. However the 0.2% proof stress can be replaced with f_{yo} for outer carbon steel tubes instead of stainless steel.

The results from formulas 8, 9 and 10 as proposed by the authors were compared with the experimental results conducted by others. The lengths of the stub columns 1 to 4 were 660 mm and the remaining 12 stub columns varied from 342 to 900 mm. The concrete cube strength was 47.9 MPa for the first four columns and 47 MPa for the other 12. The yield strengths for the first four samples were 381 and 320 MPa for the inner and outer tubes respectively. For samples 5 to 16, the yield strengths of the steel inner tube (f_{yi}) varied from 295 to 396 MPa, while that of the outer tube (f_{yo}) was either 276 or 295 MPa. As shown in Table 10, the outside tube diameters (D_o) were 114, 180, 220, 240 and 300mm and the inside tube diameters (D_i) were 48, 58, 88, 106, 114, 140, 159 and 165 mm. In Table 10, N_T represents the experimental compressive strengths from tests conducted by others and N_P represents the predicted strengths found using equations 8, 9 and 10.

Table 10 : Hassanein et al. test results

Test	$\frac{D_o}{t_o}$	$\frac{D_i}{t_i}$	f_{yi} (MPa)	f_{yo} (MPa)	N_T (kN)	N_P (kN)	$\frac{N_T}{N_P}$
1	60	16	396	276	1790	1566	1.15
2	60	29	370	276	1648	1507	1.10
3	60	47	342	276	1358	1241	1.10
4	38	19	375	295	904	881	1.03
5	80	38	295	276	2421	2261	1.08
6	100	55	321	276	3331	3092	1.08
7	150	90	290	290	2141	1807	1.19
8	75	90	290	290	2693	2429	1.11
9	92	79	397	439	5448	4849	1.12
10	176	42	221	221	635	449	1.41
11	177	84	221	221	540	411	1.32
12	177	127	221	221	378	325	1.16
13	105	26	308	308	852	651	1.32
14	105	51	308	308	728	626	1.16
15	105	76	308	308	589	551	1.06
16	74	19	286	286	968	760	1.27
17	74	36	286	286	879	750	1.18
18	74	54	286	286	704	677	1.04

The average test strength of the carbon steel CFDSCT experimental results were 16% higher than the predicted results using equations 8, 9 and 10. The test results are over-predicted by 3% to 41%. It can therefore be suggested that the proposed equations cannot predict the results of CFDSCTs very well.

2.9 Hassanein et al. (2013b)

Hassanein et al. (2013b) conducted a review on the compressive capacity of CFDSCT columns. They compared experimental research conducted by Tao et al. (2003), Lin and Tsai (2001), Li et al. (2012) and Uenaka et al. (2010) with design methodologies developed by ACI (American Concrete Institute), Han et al. (2011), Yu et al. (2013), Uenaka et al. (2010) and Hassanein et al. (2013a) to try and find the most accurate design methodologies for CFDSCT columns. They found that the spectrum of available results was not large enough and hence they modelled more columns in ABAQUS to include additional results in their study. They propose a simplified formula that predicts CFDSCTs compressive strength with greater confidence.

ACI ignores any concrete confinement effects for stub CFCT stub columns. Hassanein et al. (2013b) extended the ACI formula to include the strength component for the inner tube and hence propose the strength to be;

$$N_u = A_{so} f_{yo} + A_{si} f_{yi} + 0.85 A_c f_c^{'} \tag{11}$$

where, N_u is the axial capacity, A_{so} is the area of the outer tube, f_{yo} is the yield strength of the outer tube, A_{si} is the area of the inner tubes, f_{yi} is the yield strength of the inner tube, A_c is the area of concrete and f'_c is the cylindrical strength of the concrete. The value of 0.85 is to account for the concrete strength correlation between the stub column test and the cylindrical concrete test.

Hassanein et al. (2013b) also extended the design formula proposed by Yu et al. (2013) for CFCT stub columns. The initial proposal by Yu et al. (2013) only considered an outer tube and the concrete infill. Equation 12 includes the strength component for the inner tube;

$$N_u = \left(1 + 0.5 \frac{\zeta}{1+\zeta} \emptyset\right) \left(f_{yo} A_{so} + f'_c A_c\right) + \left(f_{yi} A_{si}\right) \tag{12}$$

where, N_u is the axial capacity, A_{so} is the area of the outer tube, f_{yo} is the yield strength of the outer tube, A_{si} is the area of the inner tubes, f_{yi} is the yield strength of the inner tube, A_c is the area of concrete and f'_c is the cylindrical strength of the concrete. ζ is the concrete confinement coefficient, which can be calculated from the Equation 13.

$$\zeta = \frac{\alpha f_{yo}}{f'_c} \tag{13}$$

The steel ratio is calculated from Equation 14

$$\propto = \frac{A_s}{A_c} \tag{14}$$

and the solid ratio can be calculated from Equation 15

$$\emptyset = \frac{A_C}{A_c + A_h} \tag{15}$$

A_h is the area of the hollow region.

The results of 18 experimental results, conducted by various researchers were compared to the five proposed design formulae and the results are shown inTable **11** Table 11. It should be noted that Hassanein et al. (2013b) adjusted the formulas developed by other authors for CFCTs by adding a strength component for the inner tubes. In Table 11, N_{TEST} represents the experimental compressive strengths from tests conducted by Tao et al. (2003), Lin and Tsai (2001), Li et al. (2012) and Uenaka et al. (2010). N_{ACI}, N_{UENAKA}, N_{HAN}, N_{YU} and $N_{HASSANEIN}$ represent the predicted strengths as proposed by the respective authors or as adjusted by Hassanein et al. (2013b) in equations 11 to 15.

Table 11 : Hassanein et al. (2013b) prediction ratios

Outer tube size	Inner tube size	f_{yo}	f_{yi}	f_{cu}	$\frac{N_{ACI}}{N_{TEST}}$	$\frac{N_{UENAKA}}{N_{TEST}}$	$\frac{N_{HAN}}{N_{TEST}}$	$\frac{N_{YU}}{N_{TEST}}$	$\frac{N_{HASSANEIN}}{N_{TEST}}$
180×3	48×3	276	370	38	0.75	1.12	0.85	0.86	0.84
180×3	88×3	276	342	38	0.81	1.03	0.89	0.90	0.88
180×3	140×3	295	375	38	0.86	0.85	0.91	0.92	0.90
114×3	58×3	276	396	38	0.79	1.01	0.88	0.91	0.97
240×3	114×3	494	297	42	0.82	1.06	0.91	0.91	0.88
300×3	165×3	221	221	19	0.83	1.01	0.92	0.90	0.85
300×2	150×3	308	308	19	0.79	0.94	0.86	0.87	0.78
300×4	180×2	290	290	22	0.81	0.99	0.89	0.93	0.85
350×3.8	231×2.9	221	221	19	0.82	0.92	0.89	0.90	0.83
158×0.9	38×0.9	286	286	19	0.64	0.91	0.72	0.71	0.67
159×0.9	76×0.9	286	286	19	0.71	0.90	0.78	0.77	0.73
159×0.9	114×0.9	286	286	19	0.84	0.90	0.90	0.89	0.83
158×1.5	39×1.5	221	221	19	0.66	1.04	0.73	0.78	0.74
158×1.5	77×1.5	308	308	19	0.77	1.01	0.84	0.89	0.84
158×1.5	114×1.5	308	308	19	0.90	0.93	0.95	0.98	0.92
158×2.1	40×2.1	276	321	38	0.67	1.09	0.74	0.81	0.76
158×2.1	77×2.1	290	290	22	0.76	1.00	0.82	0.88	0.83
157×2.1	115×2.1	276	295	38	0.91	0.93	0.96	1	0.95

When the adjusted equation from ACI is compared to the test results, it was found that it underestimated the strength by up to 36%. This is a result of not considering any effects of concrete enhancement. The formulae by Yu et al. (2013) predicted the strength fairly well, for diameter-to-thickness ratios of 47 to 150. Hen et al. (2011) also predicted the strengths reasonably well, for diameter-to-thickness ratios of less than 150.

Current research has a limited diameter-to-thickness range, with few tests having a ratio of less than 47 or greater than 150. Hence the authors modelled 36 CFDSCTs with varying parameters to achieve more results in order to understand the behaviour of CFDSCTs more comprehensively. In order to validate the finite element model, test results were compared to those found by finite element analysis. In Table 12, N_{FE} represents the compressive strength found by finite element analysis and N_T represents the experimental strengths found by Tao et al. (2004), Lin and Tsai. (2001) and Li et al. (2012).

Table 12 : Hassanein et al. predicted vs. test ratios

Test	N_{FE} (kN)	N_T (kN)	$\frac{N_{FE}}{N_T}$
1	1728	1790	0.97
2	1570	1648	0.95
3	2048	2141	0.96
4	2590	2693	0.96
5	5280	5448	0.97

From Table 12 it can be seen that there is good agreement between the test results and the FE predicted results.

The CFDSCTs were modelled in ABAQUS with a mesh size of 25mm. End plates were modelled to simulate uniform loading on the columns. Load was applied to the top cover plate. The friction coefficient was set to 0.4 between the concrete and steel tube. The yield value stated in the literature review was 235 MPa and the compressive strength of the concrete was 40 MPa.

Table 13 : Hassanein et al. test results

Test	D_o (mm)	D_i (mm)	$\frac{D_o}{t_o}$	$\frac{D_i}{t_i}$	N_T (kN)
1	300	150	47	15	5279
2	300	150	38	15	6407
3	300	150	30	15	7171
4	300	150	25	15	7830
5	300	150	21	15	8552
6	400	200	47	20	8203
7	400	200	40	20	9939
8	400	200	33	20	11015
9	400	200	29	20	12013
10	400	200	25	20	12927
11	500	250	47	25	13064
12	500	250	42	25	14150
13	500	250	36	25	15502
14	500	250	31	25	16784
15	500	250	28	25	18043
16	600	300	47	30	18005
17	600	300	43	30	19190
18	600	300	38	30	20925
19	600	300	33	30	22380
20	600	300	30	30	24201
21	300	150	155	15	3268
22	300	150	165	15	3205
23	300	150	175	15	3181
24	300	150	185	15	3170
25	400	200	155	20	5227
26	400	200	165	20	5194
27	400	200	175	20	5159
28	400	200	185	20	5098
29	500	250	155	25	7780
30	500	250	165	25	7704
31	500	250	175	25	7638
32	500	250	185	25	7579
33	600	300	155	30	10789
34	600	300	165	30	10689
35	600	300	175	30	10596
36	600	300	185	30	10433

The finite element results were compared to the formulas proposed by ACI (American Concrete Institute), Han et al. (2011), Yu et al. (2013), Uenaka et al. (2010) and Hassanein et al. (2013a). They found that Hassanein et al. (2013a) predicted the strengths most accurately for diameter-to-thickness ratios of less than 47. They also found that when the diameter-to-thickness ratio was greater than 150 than Equation 11 (adjusted ACI equation) predicted the strength most accurately.

Based on these results, Hassanein et al. (2013b) proposed a new formula that has two diameter-to-thickness bounds. For a diameter-to-thickness ratio less than 150 they propose Equation 16.

$$P = \left(1 + 0.3\frac{\emptyset}{\emptyset + 1}\theta\right)\left(f_{sye}A_{se} + f'_{cc}A_{sc}\right) + \left(f_{syi}A_{si}\right) \quad (16)$$

Equation 16 above suggests that no concrete confinement is provided by the inner tube. The outer tube alone provides concrete confinement. For diameter-to-thickness ratios greater than 150, they proposed Equation 17.

$$P = f_{sye}A_{se} + 0.85f'_{c}A_{sc} + f_{syi}A_{si} \quad (17)$$

Equation 17 suggests than no enhancement factor is achieved for diameter-to- thickness ratios greater than 150. The same formula as proposed by ACI is reproduced. The research concludes with a final recommendation that axially loaded slender CFDSCT columns need to be researched, as no literature is available in this research area.

2.10 Summary

This chapter provides a review of the literature available on CFDSCT columns. The stub columns are intended to give guidance for the design of long columns. Important aspects of each paper are covered, which include the specimen dimensions and properties, failure modes, effects of confinement, test results and the proposed design formulations. As expected, the mode of failure of the outer tubes was outward local buckling. It was also found that the inner tubes of some CSDSCT failed by inward local buckling and shear of the concrete infill. This was common in inner tubes with larger diameter-to-thickness ratio. The availability of concrete confinement varied from author to author. Tao et al. (2004) results suggest that there is no enhancement; Uenaka et al. (2010) results suggest that confinement ranges from 0 to 41%, and Wei et al. (1995) results suggest that test specimen have an average of 15% confinement. Based on the discussions above it is inconclusive to judge whether there is useful confinement in CFDSCT or not. Hence it is proposed that research is conducted on intermediate to slender CFDSCT columns. The results found from the tests will be used to formulate proposals for implementation in SANS 10162-1 and EC4.

3. Experimental Programme

3.1 Introduction

The aim of this chapter is to explain how the columns were prepared from the inception stage until they were ready for testing. This includes the column preparation, concrete property testing, steel property testing, column testing, instrumentation and precautions to ensure accurate results were achieved.

3.2 Scope of samples tested

The columns comprised two steel tubes and a sandwiched layer of concrete. All the inner steel tubes had a diameter of 76.2 mm and a wall thickness of 2 mm. This diameter of inner tube was specifically chosen so that it would simulate a 75 mm pipe, as commonly used in industry as a downpipe. The diameters of the outer steel tubes selected were 139.2, 152.4, 165.1 and 193.7 mm. The upper bound of these diameters was chosen so that they represent the sections used in practice and the lower bound was chosen to accommodate the 19 mm stones in the wet concrete. All the outer tubes had a wall thickness of 3 mm, with the exception of the 193.7 mm tube, which had a wall thickness of 3.5 mm. The outer tubes had diameter-to-thickness ratios of between 46 and 55. This range was selected based on the maximum diameter to thickness ratios set for CFTs in SANS 10162-1 and EC4. Although CFDSCTs are different for CFTs, these values are used for guidance in respect of what is used in engineering practice. SANS 10162-1 and EC4 specify maximum outer diameter-to-thickness ratios to avoid local buckling of CFTs. Hence, it was expected that the CFDSCTs will fail by overall buckling only. All the steel tubes were supplied by Macsteel and conformed to SANS 657-1 for cold steel.

The columns were prepared in lengths of 1.0, 1.5, 2.0 and 2.5 m. These lengths were specifically chosen to establish the strength of these sections over a wider range of slenderness. A total number of 64 steel tubes were used to fabricate 32 columns. The columns were fabricated in pairs of 16 different sections. Figure 5 shows the typical cross-sections and Table 14 shows the dimensions of the tubes tested. In Table 14, L_T is the theoretical length of the column, L_a is the actual length of the column, D_o is the outer

tube diameter, D_i is the inner tube diameter, t_o is the outer tube thickness and t_i is the inner tube thickness.

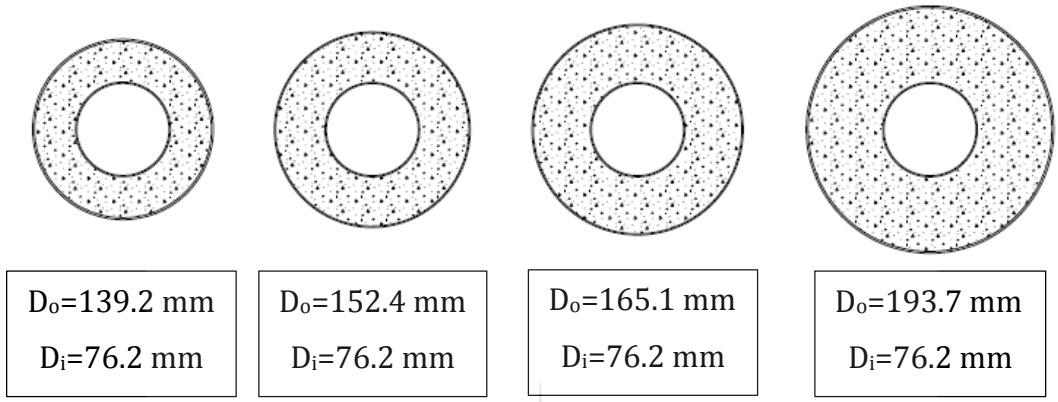

Figure 5 : CFDSCTs with outer and inner diameters

Table 14 : Dimensional properties of columns

Specimen	L_t (mm)	L_a (mm)	D_o (mm)	t_o (mm)	D_i (mm)	t_i (mm)	$\frac{D_o}{t_o}$	$\frac{D_i}{t_i}$
1	1000	998	139.2	3	76	2	46	38
2	1000	1001	139.2	3	76	2	46	38
3	1500	1500	139.2	3	76	2	46	38
4	1500	1503	139.2	3	76	2	46	38
5	2000	2000	139.2	3	76	2	46	38
6	2000	1998	139.2	3	76	2	46	38
7	2500	2502	139.2	3	76	2	46	38
8	2500	2498	139.2	3	76	2	46	38
9	1000	1003	152.4	3	76	2	51	38
10	1000	1002	152.4	3	76	2	51	38
11	1500	1497	152.4	3	76	2	51	38
12	1500	1503	152.4	3	76	2	51	38
13	2000	1997	152.4	3	76	2	51	38
14	2000	2000	152.4	3	76	2	51	38
15	2500	2498	152.4	3	76	2	51	38
16	2500	2500	152.4	3	76	2	51	38
17	1000	998	165.1	3	76	2	55	38
18	1000	999	165.1	3	76	2	55	38
19	1500	1504	165.1	3	76	2	55	38
20	1500	1498	165.1	3	76	2	55	38
21	2000	2003	165.1	3	76	2	55	38
22	2000	1998	165.1	3	76	2	55	38
23	2500	2498	165.1	3	76	2	55	38
24	2500	2502	165.1	3	76	2	55	38
25	1000	1003	193.7	3.5	76	2	55	38
26	1000	1000	193.7	3.5	76	2	55	38
27	1500	1502	193.7	3.5	76	2	55	38
28	1500	1500	193.7	3.5	76	2	55	38
29	2000	1998	193.7	3.5	76	2	55	38
30	2000	2003	193.7	3.5	76	2	55	38
31	2500	2503	193.7	3.5	76	2	55	38
32	2500	2497	193.7	3.5	76	2	55	38

3.3 Steel coupon tests

A total of 15 coupons were prepared and tested. The results sought from the tensile tests were the 0.2% yield stress and strain, the ultimate tensile stress and Young's modulus of elasticity. For each of the different diameters of inner and outer tubes, 3 coupon tests were conducted.

The coupons were produced by cutting material from the steel tubes. The material was then flattened. The flattened metal sheets were cut into strips of exactly 200 by 25 mm sizes as shown in Figure 6. The strips were cut using a Keetona guillotine as shown in Figure 8. The guillotine was specifically used for this task because it produces an absolutely straight and accurate cut edge. This is necessary because a high level of accuracy is required for the coupons since the stress-strain test is sensitivity to dimensional tolerances. The steel strips were machined in a Nicolas Correa machine such that they had a gauge width of 15 mm. The widths were measured accurately using a pair of venier calipers, with a needle dial, and then input into the Instron computer.

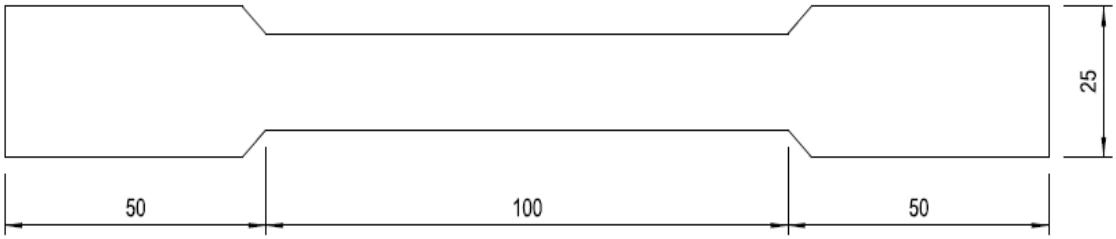

Figure 6: Tensile coupon dimensions

Figure 7 : Photograph of coupons

Figure 8 : Keetona guillotine

The tensile tests were conducted in an Instron 1195 (as shown in Figure 9) with a maximum capacity of 100 kN at the Materials Laboratory at the University of Johannesburg. The coupons were all carefully aligned and properly clamped in the grips. Correct alignment is of importance since incorrect alignment can lead to premature failure due to the undesirable bending stresses. Improper clamping can lead to slippage of the coupon and lead to a failure of the test.

Figure 9 : Instron 1195

The coupons were loaded at a rate of 3 mm/min. Selecting the correct rate of loading is important because it could affect the strain results. The output data from the computer were strain and stress. These were plotted so that the yield stress, ultimate stress and modulus of elasticity could be established.

As shown in Figure 10, an extensometer was used to measure the strain. It was imperative to use an extensometer since the strains are too small to be accurately measured by the Instron load data logger. The individual and average material properties are presented in Table 15 and 16. The stress vs. strain graphs are plotted in Figure 11 to 15.

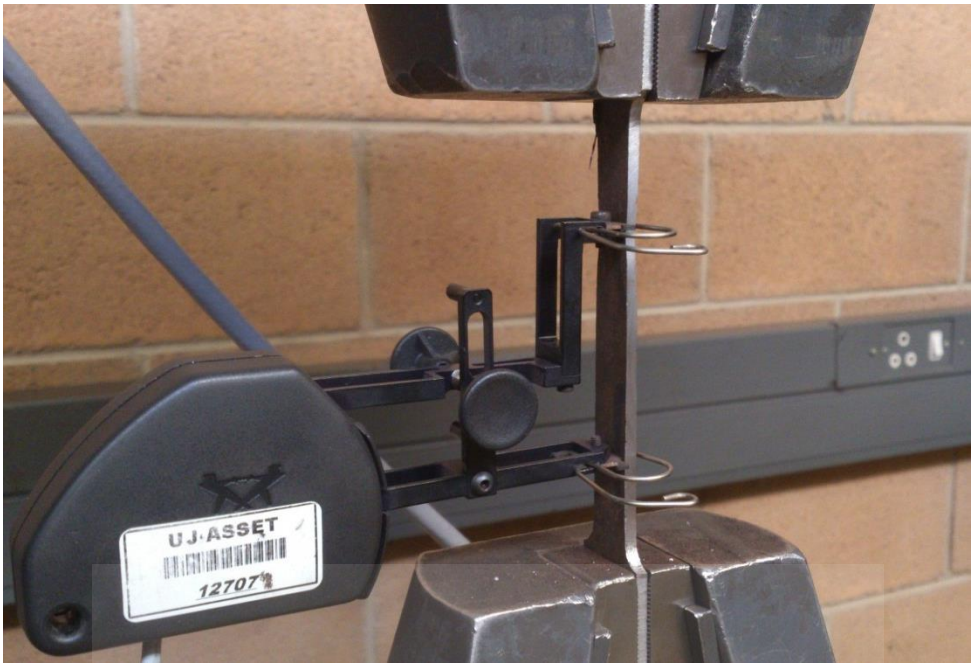

Figure 10 : Steel coupon with extensometer

Table 15: Individual CHS coupon test results

Tube Diameter (mm)	Sample number	f_y (MPa)	f_u (MPa)	E_s (MPa)
76.2	1	323.12	373.41	200213
	2	319.16	362.74	204348
	3	329.01	384.23	210313
139.7	1	409.97	498.37	202505
	2	417.07	495.49	203652
	3	426.18	509.89	203541
152.4	1	544.03	550.46	207304
	2	552.46	575.35	205388
	3	549.86	584.61	205967
165.1	1	519.36	577.09	205967
	2	513.67	586.48	202312
	3	515.33	579.95	202312
193.7	1	392.20	470.80	206800
	2	393.53	485.10	209977
	3	388.03	482.13	207109

Table 16: Average CHS coupon test results

Tube Diameter (mm)	f_y(MPa) average	f_u(MPa) average	E_s(MPa) average
76.2	324	373	204958
139.7	418	501	203233
152.4	549	570	206220
165.1	516	581	203530
193.7	391	479	207962

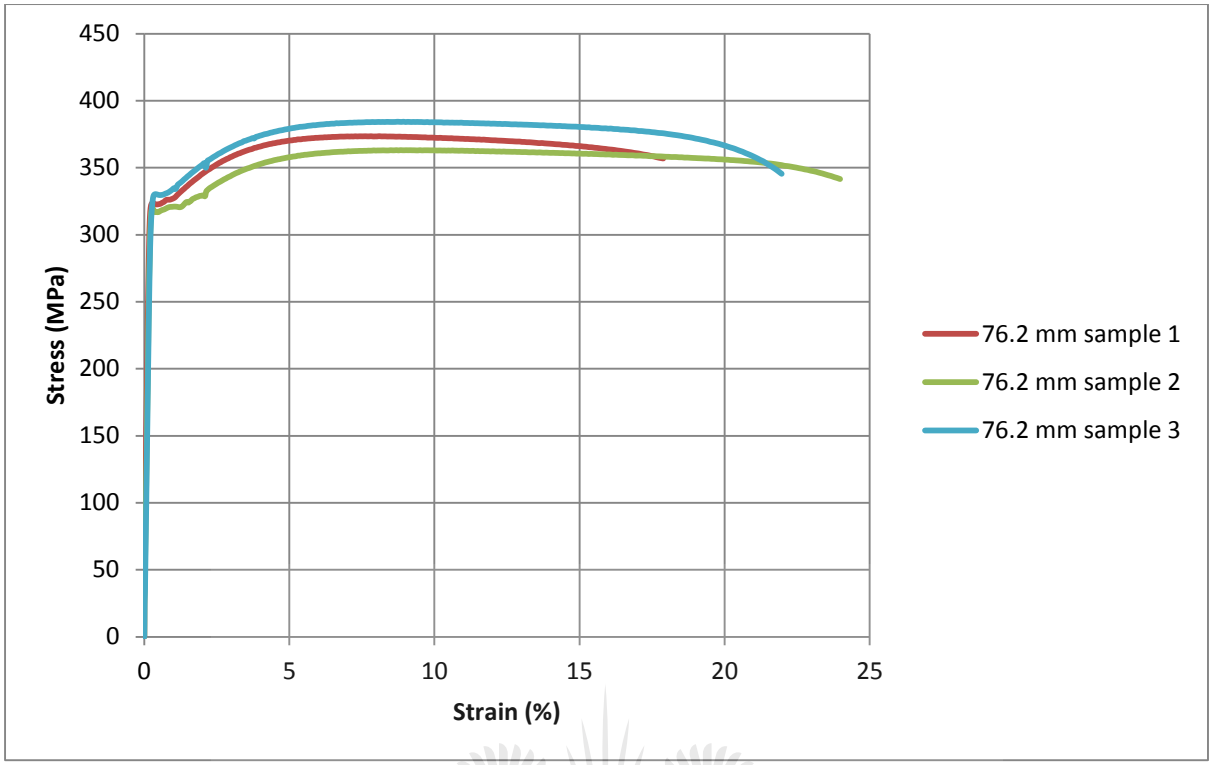

Figure 11: Stress vs. Strain results for 76.2 mm CHS

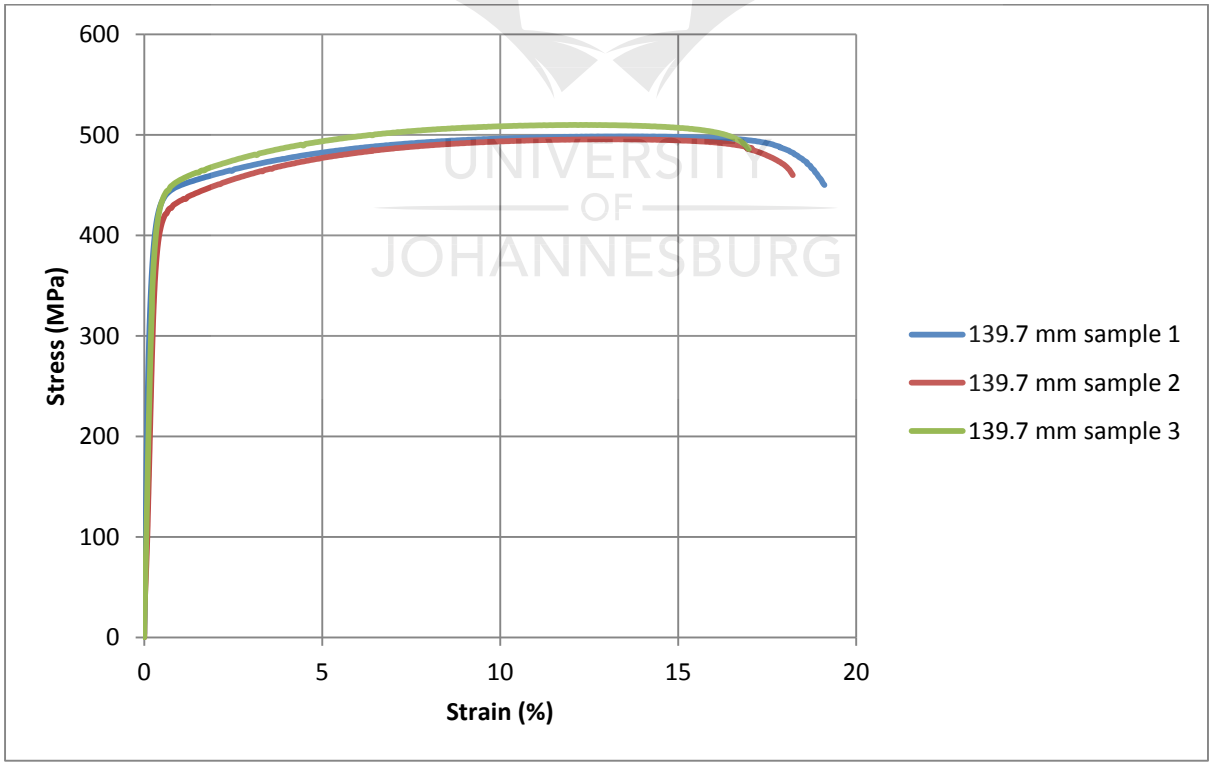

Figure 12: Stress vs. Strain results for 139.7 mm CHS

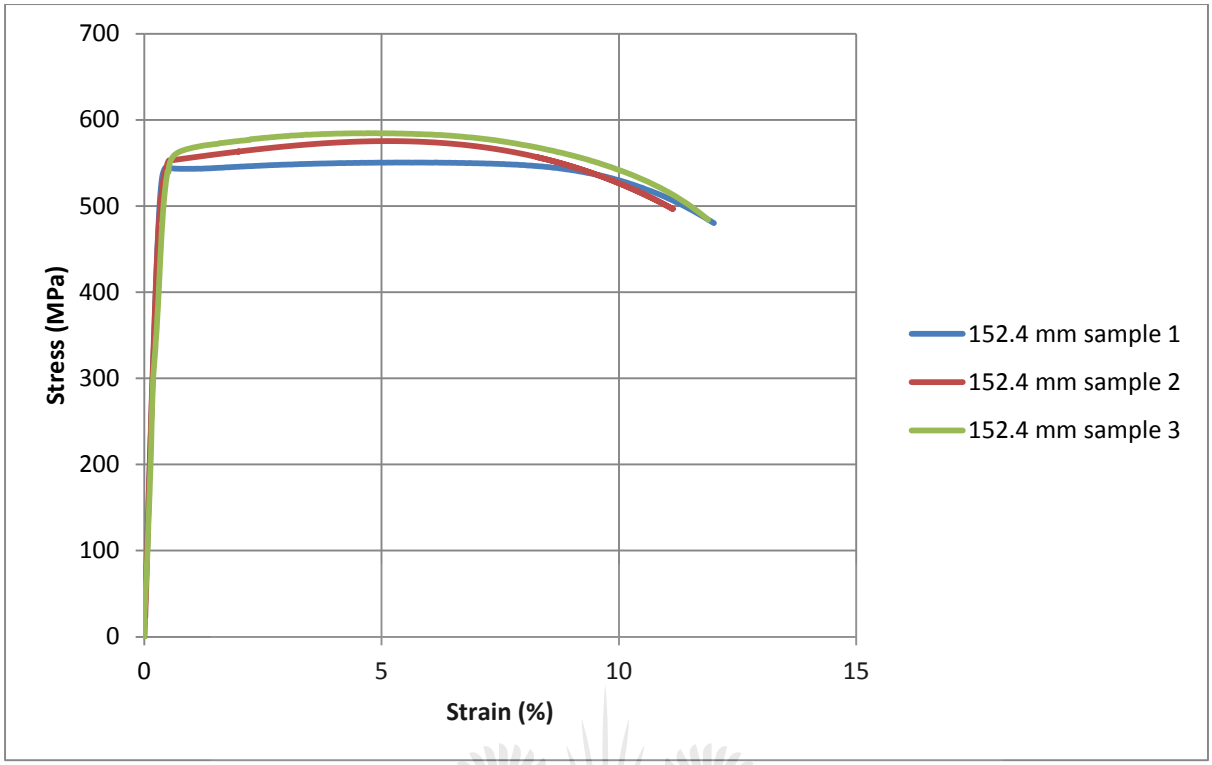

Figure 13: Stress vs. Strain results for 152.4 mm CHS

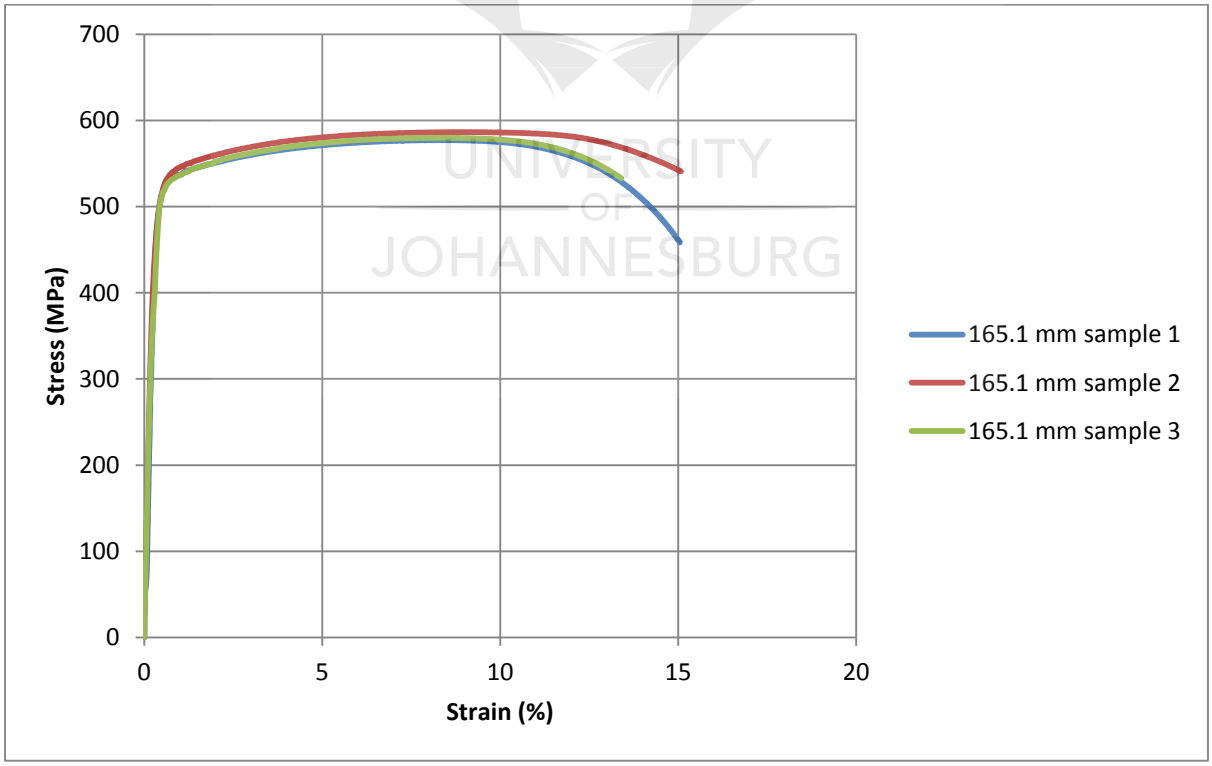

Figure 14 : Stress vs. Strain results for 165.1 mm CHS

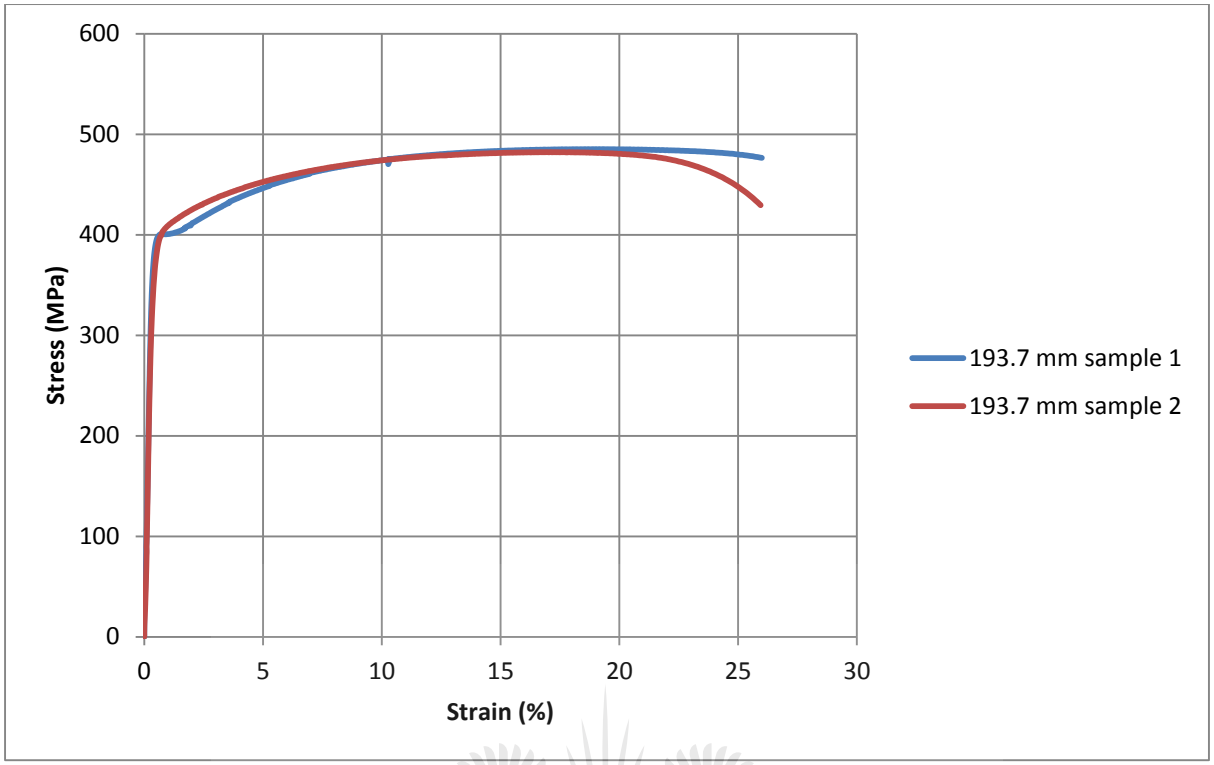

Figure 15 : Stress vs. Strain results for 193.7 mm CHS

3.4 Concrete cube tests

The concrete ordered for this experiment was 30 MPa with 19 mm stone. SANS 10162-1 and EC4 specify that the strength of concrete for CFTs must range from 25 MPa to 100 MPa and 20 MPa to 50 MPa respectively. Further to this, 30 MPa concrete is commonly used in South Africa for the construction of columns. Low concrete strength also promotes maximum ductility.

The concrete used in this experiment was generously sponsored by Pronto Mix. As shown in Figure 16, batching of the concrete took place in the lab. The total volume of concrete required for the experiment was 0.95m^3. However, approximately 20% extra was ordered for casting cubes and wastage.

Figure 16 : Ready-mix concrete truck

The cube tests were conducted in accordance with SANS 5860:2006. Six concrete cubes of 100 × 100 × 100 mm size were cast as shown in Figure 17. The tolerance required by SANS 5860:2006 is ± 1 % on all the dimensions of the cube. All the cubes were measured and were within the required tolerance. SANS 5860:2006 further requires that the cube size must be at least 4 times larger than the aggregate size. The aggregate size was 19 mm hence this requirement was satisfied.

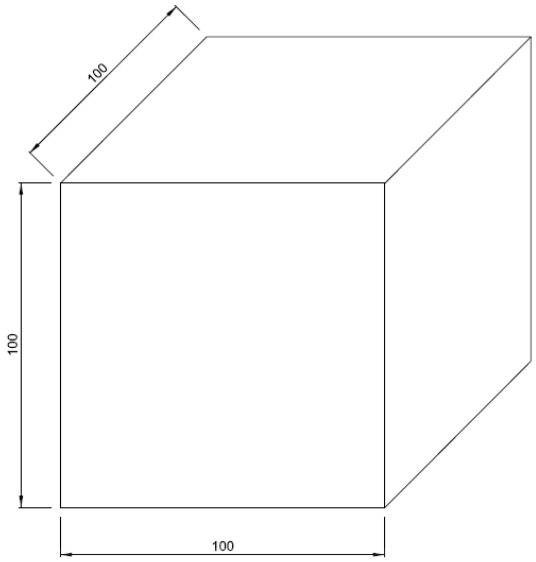

Figure 17 : Cube dimensions

The cubes were cast and were compacted using a vibrating table. This was done in accordance with clause 4.1.3 as specified in SANS 5861-3:2006. The cubes were then cured at the University of Johannesburg in a temperature controlled bath as per the specifications in clause 4.2 of SANS 5861-3:2006. The cubes were removed from the bath and tested in a Tinius Olsen machine at the University of Witwatsrand. Figure 20 shows the Tinius Olsen Machine. The concrete cube crushing was done at 28 days. Figure 21 shows a crushed concrete cube. The cubes were inspected for honeycombing, excess voids, levelness and broken corners. None of these deformities were found in the cubes. The failure of the cubes showed that the exposed surfaces were all cracked, hence indicating that the cubes failed in a satisfactory manner. Refer to Figure 19 for the modes of failure of concrete cubes. The cube results are presented in Table 17.

Figure 18 : Temperature controlled bath

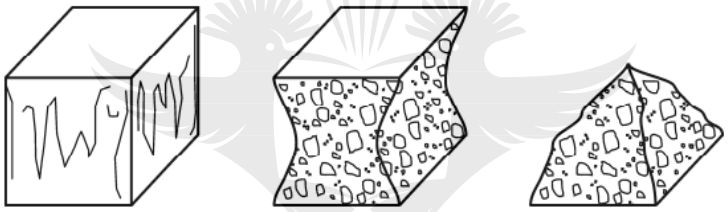

Satisfactory modes of failure: All four surfaces are cracked approximately equally

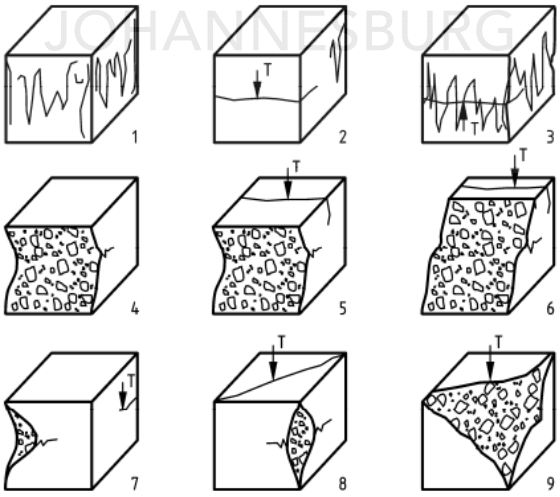

Unsatisfactory modes of failure

Figure 19 : Modes of failure of concrete cubes (adapted from EN 12390-3:2009)

Figure 20 : Concrete cubes tested in Tinius Olsen

Figure 21: Crushed concrete cube

Table 17: Concrete cube properties

	Mass (g)	Density (kN/m^3)	Failure load (kN)	Cube strength (MPa)	Modulus of Elasticity (GPa)
Sample 1	2495	24.95	308.8	30.9	28.27
Sample 2	2465	24.65	333.6	33.4	29.02
Sample 3	2425	24.25	308.9	30.9	28.27
Sample 4	2420	24.2	301.2	30.1	28.03
Sample 5	2413	24.13	285.8	28.6	27.44
Average	2444	24.44	307.7	30.8	28.21

The average strength of the cube tests is 30.8 MPa, and all the results in Table 17 are comparable to the 30 MPa concrete strength ordered. The Modulus of elasticity was determined using Table 1 of SANS 10100-1. The cube strengths are converted to their respective modules between a range of values using interpolation. The table was used instead of the formula under section 3.4.2.1.1, because the formula only caters for concrete with a density below 22 kN/m^3.

3.5 Construction of columns

The inner and outer steel tubes were first cut to their correct sizes. They were cut in a Ercole 360S horizontal band saw as shown in Figure 22. Water was continuously sprayed to ensure that the heat generated during the cutting process did not damage the tubes. The heat could cause uneven expansion and contraction on the cutting surfaces and hence induce undesired stresses or even cause warping of the plate material. The tubes were in 8 m lengths, hence their method of support during the cutting process was important. Incorrect support could cause the tubes to move out of their plane, hence causing deformation effects of initial out of straightness. Part of the parameter "n" in SANS 10162-1 deals with initial out of straightness and hence it is imperative that the tubes were not subjected to external forces that could cause deviation from the centroid. The tubes were supported by trestles with rollers at a minimum of 2 m apart during the cutting process. The tubes were not in any situation cantilevered, instead they were simply supported in all situation. The worst case set-ups is shown in Figure 23.

Figure 22 : Erocle 360S horizontal band saw

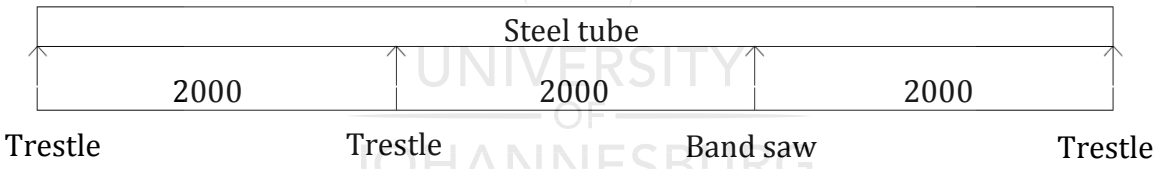

Figure 23 : Tube supports during cutting

8 mm thick base plates were cut from a large metal sheet to practical sizes to match the outer column diameters. The exact positions of the tubes were traced on the plates using a permanent marker. The inner tubes were than tack welded on their marked positions as shown in Figure 24. There after the outer tubes were placed on their marked positions and were also tack welded. It was imperative to only tack weld the tubes and not continuously weld the tubes as a continuous weld could have caused premature failure at the base plate hence defeating the purpose of the test. In order to ensure the correct distance between the tubes, Styrofoam spaces were used. The distance between the top of the tubes were then measured to ensure that the space between the tubes were correct. The final check was conducted using a spirit level to ensure that the columns were level.

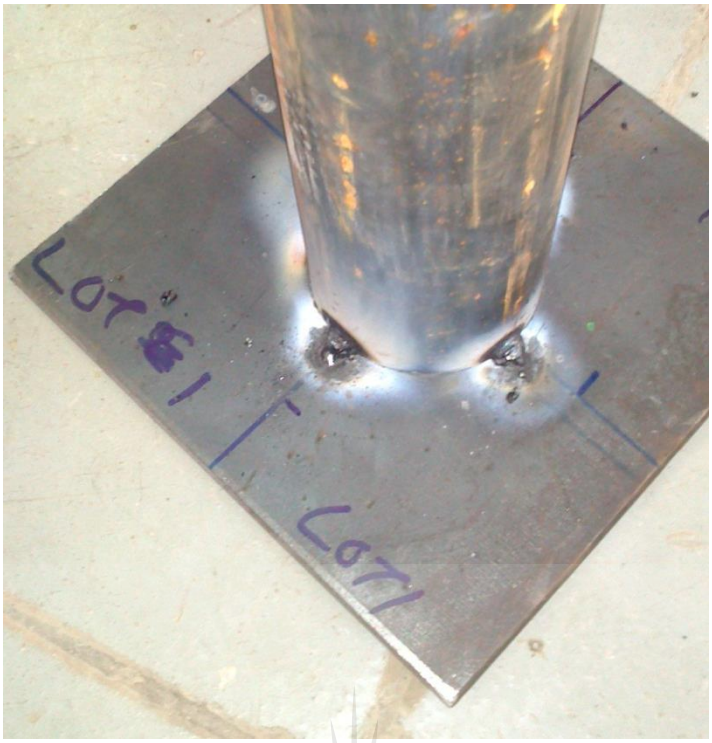

Figure 24: Steel tubes tack-welded to base plate

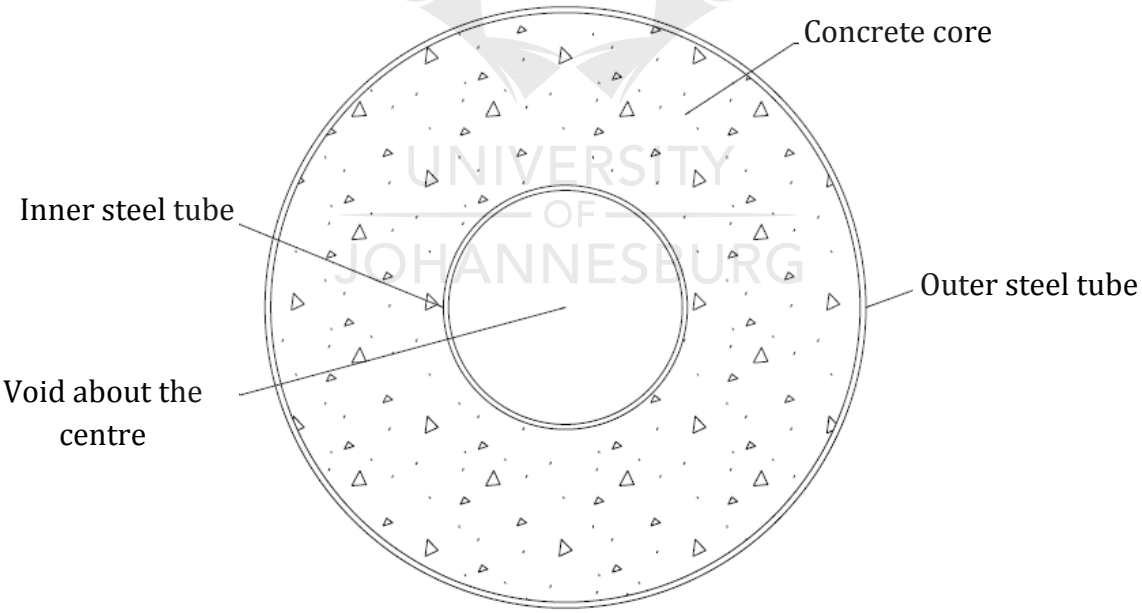

Figure 25: Cross-section of composite column

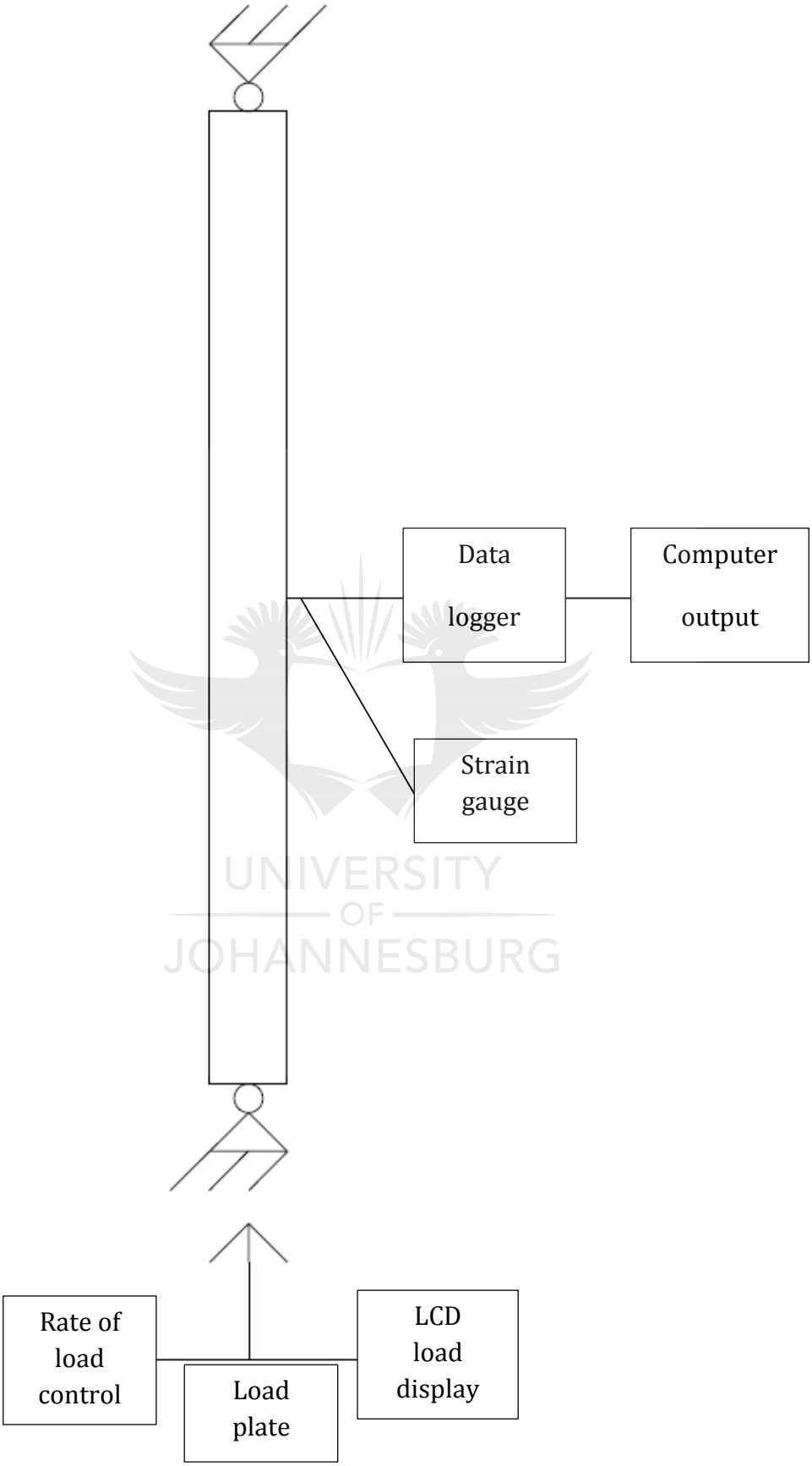

Figure 26 : CFDSCTs load test setup

The ready-mix concrete was batched in small quantities and four personnel filled the tubes with concrete. It was necessary for four people to carry out this activity as the columns needed to be filled quickly in order to prevent the concrete from setting.

During the filling process, the concrete was also vibrated. The 1 and 1.5 m length columns were vibrated using a vibrating table as shown in Figure 27. These columns were held in position on the table to ensure that they did not move off the table. The 2 and 2.5m length columns were too long and heavy to place on the vibrating table. They were vibrated using long temping rods and also a poker vibrator. All casting and vibrating took place at the University of Johannesburg.

Concrete was cast above the top of the columns and excess concrete was trimmed off using a grinder with a diamond blade. Extreme care was taken during the grinding process to ensure that the top surface, which would be used as a loading surface, was level. This was done to ensure that the entire steel and concrete cross sectional area was equally loaded when the columns were crushed. Due to the trimming, the final column heights differed from one another by a few millimetres. The final column heights are as listed in Table 14.

Figure 27: Columns on vibrating table

3.6 Test setup

All the columns were transported and tested at the University of Witwatersrand in the Civil Engineering Laboratory. Strain was measured using strain gauges. As shown in Figure 32, four strain gauges were attached to each column at mid-height.

The strain gauges were purchased from Rocklab. The gauge length is defined as the length of the grid in the direction of the measurement on the specimen. The longer the strain gauge the greater the length the average strain is measured over. For concrete, longer steel gauges (greater than 30 mm) are required. However, since the strain gauge was attached to the steel, 10 mm was chosen. The resistance of the strain gauges were 120 ohms.

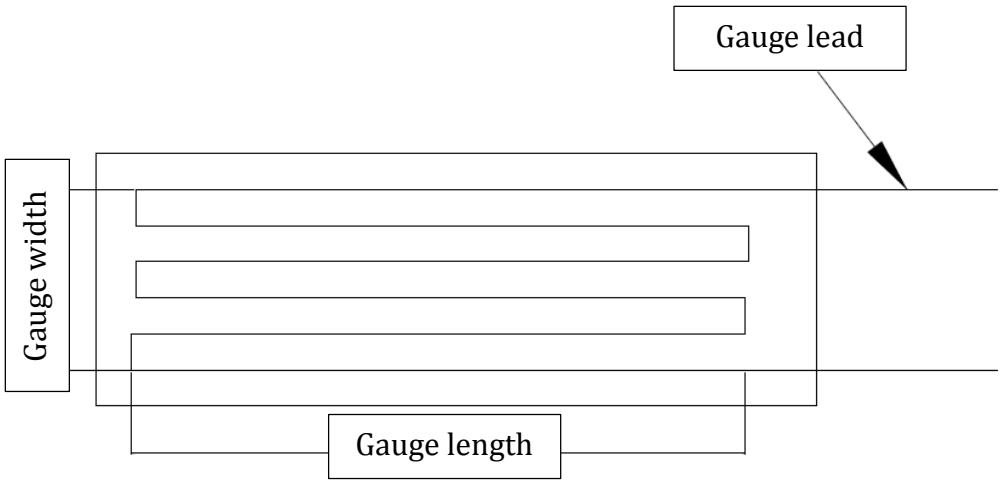

Figure 28 : Strain Gauge

It is very important to correctly apply the strain gauges, in order to get accurate results. The locations for the strain gauges were measured and marked with a marker on all four sides. The area cleaned was a square with dimensions of approximately 3 cm by 3 cm. Before attaching the strain gauges, surface contaminants were removed from the columns using a wire brush. This area was then cleaned with ethanol. The gauges were attached immediately to the tube, using an adhesive, since any delays could cause new contaminants to settle. One drop of adhesive was applied which was then spread as a uniform thin layer. The gauges were then positioned on their specified locations with pressure and allowed to cure. Surgical gloves were used to ensure that no oils or other foreign contaminants came into contact with the strain gauges or the applied surface. The gauge leads were connected to silicon board contact terminals just below the strain gauge. The silicon boards were also attached to the columns using adhesive. The gauge leads were soldered to the logging wires on the silicon boards. The wires were connected to the logging equipment. Extreme care and precaution was taken when attaching the strain gauges to ensure they did not get damaged. Any damaged strain gauges were removed and the preparation processes was repeated before the new strain gauge was attached. The strain gauges were then connected to a National Instruments data logger. The strain gauges were tested to ensure that they had the required resistivity. During loading, the data was fed into the computer via the data logger.

The columns were tested in the Langen Hausen Machine as shown Figure 29, with the exception of columns 25, 26, 27 and 28 (1 and 1.5 m long columns with 193.7 mm diameters) which were tested in the Amsler Machine as shown in Figure 30. The

maximum load capacity of the Langen Hausen and Amsler were 1700 kN and 2500 kN respectively. Both machines were calibrated by IMP calibration services. The rationale behind testing columns 25 to 28 in a different machine was that the predicted strengths exceeded the maximum capacity of the Langen Hausen, while the Amsler could not be used to test all the columns due to the maximum height restriction of 2 m.

Figure 29 : Langen Hausen testing machine

Figure 30 : Amsler testing machine

Figure 31: Typical test set-up

The rate of loading used was 3 mm/min. The loading was applied constantly. The compressive load readings were logged manually at 5 second intervals. The values from the Langen Hausen were read off a digital LCD screen and the values from the Amsler were read off an analogue dial.

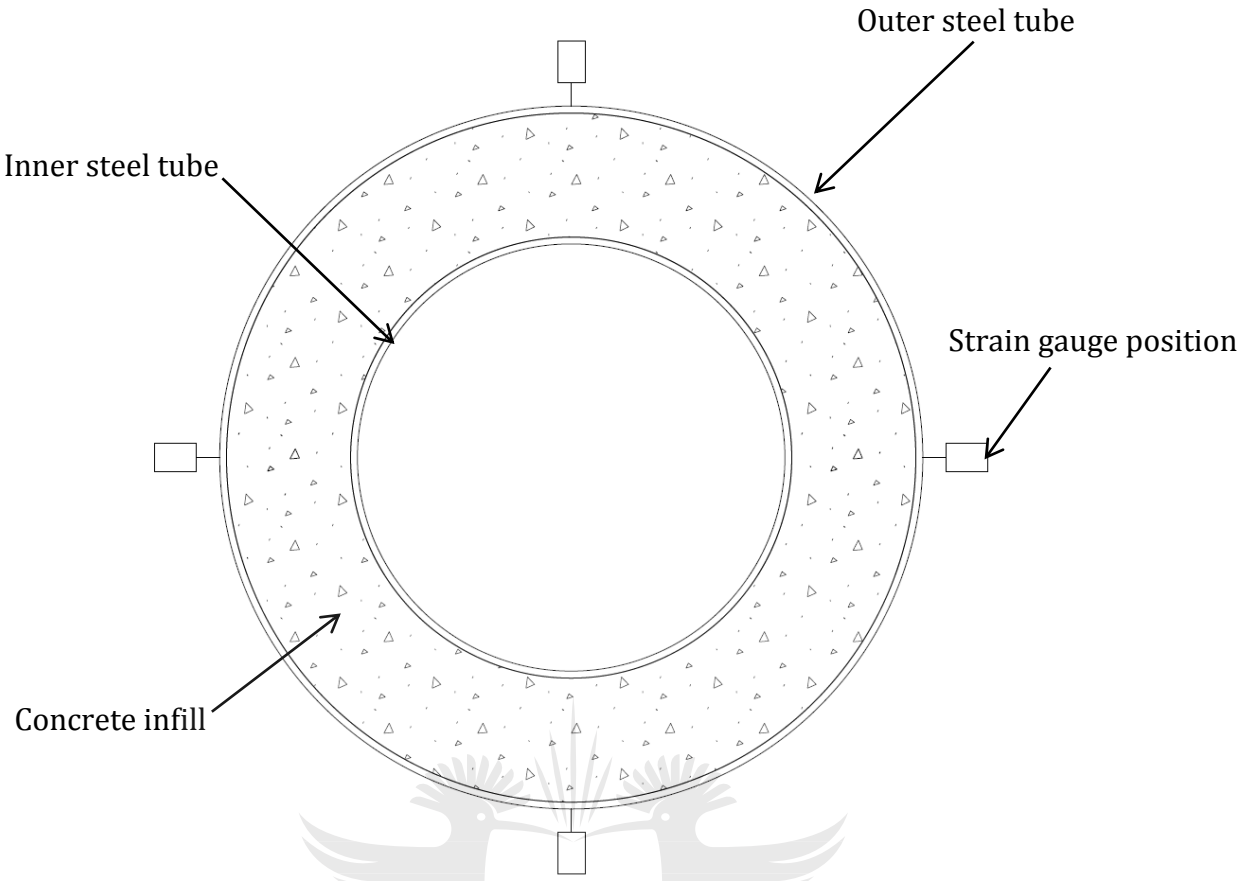

Figure 32: Arrangement of Strain Gauges

In order to determine the failure of the inner tube, a Sony Xperia Sola video camera was used. The camera was lowered into the inner tubes and a video footage was recorded at defined height intervals. A measuring tape was fixed in the inner tube during the test. The video footage had the measuring tape marking on it as it was viewed, hence the exact location of damage could be identified. A naked eye observation was also conducted with the aid of a torch.

4. Experimental Results

4.1 Introduction

The purpose of this chapter is to present and discuss the results that were obtained from the experiments. The modes of failure are also discussed. The experimental ultimate capacities of the columns are used to develop the formulae for estimating the axial load capacity for CFDSCTs.

4.2 Mode of failure

The CHS outer tubes of 1 m lengths failed by a combination of overall buckling and yielding of the steel tube. All the yielding occurred in the upmost region of the column. The outer steel tube failed by bulging outward as shown in

Figure 33. Tao et al. (2004), Uenaka et al. (2009), and Wei et al. (1995) also found the outer tubes to buckle outwards. Hence this mode of failure is consistent with the failure pattern of short columns found by other authors. However, Tao et al. (2004) and Wei et al. (1995) found that the bulging occurred at mid-height of the stub column, while Uenaka et al. (2009) found the buckling to occur in the top half of the columns. The difference in the location of the local buckle can be attributed to the fact that the short columns considered in this research are almost double the height of the columns tested by these researchers.

Uenaka et al. (2010) and Wei et al. (1995) found that their inner tubes failed by inward buckling. The diameter-to-thickness ratios for the inner tubes in this research ranged from 19 to 146. Tao et al. (2004), however, found that the inner tubes with larger diameter-to-thickness ratios failed by inward buckling, whilst those with smaller diameter-to-thickness ratios showed no sign of local buckling. In this investigation no local buckling was found, hence this agrees with the findings of Tao et al. (2004).

The 1.5, 2.0 and 2.5 m double-skin columns failed by overall buckling only. This can be seen in Figure 34. The tubes behaved as predicted by Euler (Hibbler, 2006), as the maximum displacement was at mid-height. No comparison can be made to previous researchers as they have not tested intermediate to slender CFDSCTs.

Figure 33: Bulging of 1m length tubes

(a) Intermediate column (b) Slender column

Figure 34: Overall buckling

4.3 Change in final diameter of columns

After the test, the diameters of the columns were measured to determine any change in size of the diameters. A noticeable increase in the diameter was found only in the 1 m length columns. In the 1 m length columns for the 139, 152, 165 and 193 mm outside tube diameters, the average change in diameters were 4, 3, 5 and 8mm respectively.

The change in diameter of the outer tubes of 1 m length columns is an important finding. It suggests that the outer tube resists circumferential stresses, caused by the expansion of concrete. Based on this finding, it can be postulated that an enhancement factor can be applied to the concrete core and a reduction factor be applied to the outer steel tube. This behaviour is similar to ordinary concrete-filled tubes.

4.4 Load and strain

Typical axial load versus vertical strain results are plotted in Figures 35 to 38. Figures 35 and 36 consist of load versus strain graphs for columns of the same diameters but different lengths. The curves plotted in figures 37 and 38 are for columns with the same lengths but different diameters.

It can be noted from Figures 35 to 38 that the load-strain behaviour was initially linear. During this phase of the graph the steel tubes act independently from the concrete fill because the poisson's ratio of the steel tube is higher than that of the concrete.

The graph then becomes inelastic (non-linear) towards the ultimate load limit. This behaviour is caused by a combination of the yielding of the steel and the expansion of the concrete infill. The expansion of the concrete causes hoop stresses to develop in the steel tubes. Since the steel section already resist longitudinal stresses from the applied load, the introduction of additional stresses (hoop or circumferential stresses) reduces the strength of the tube. The reduction in the steel tube strength and an increase in the concrete strength is maintained until the steel tubes cannot sustain the load any longer. In the case of short columns, this would result in local buckling and in long columns this would result in overall buckling. All the columns showed significant ductility till failure. As shown in Figures 35 to 38, ductility is more significant in specimens with larger diameters and shorter lengths.

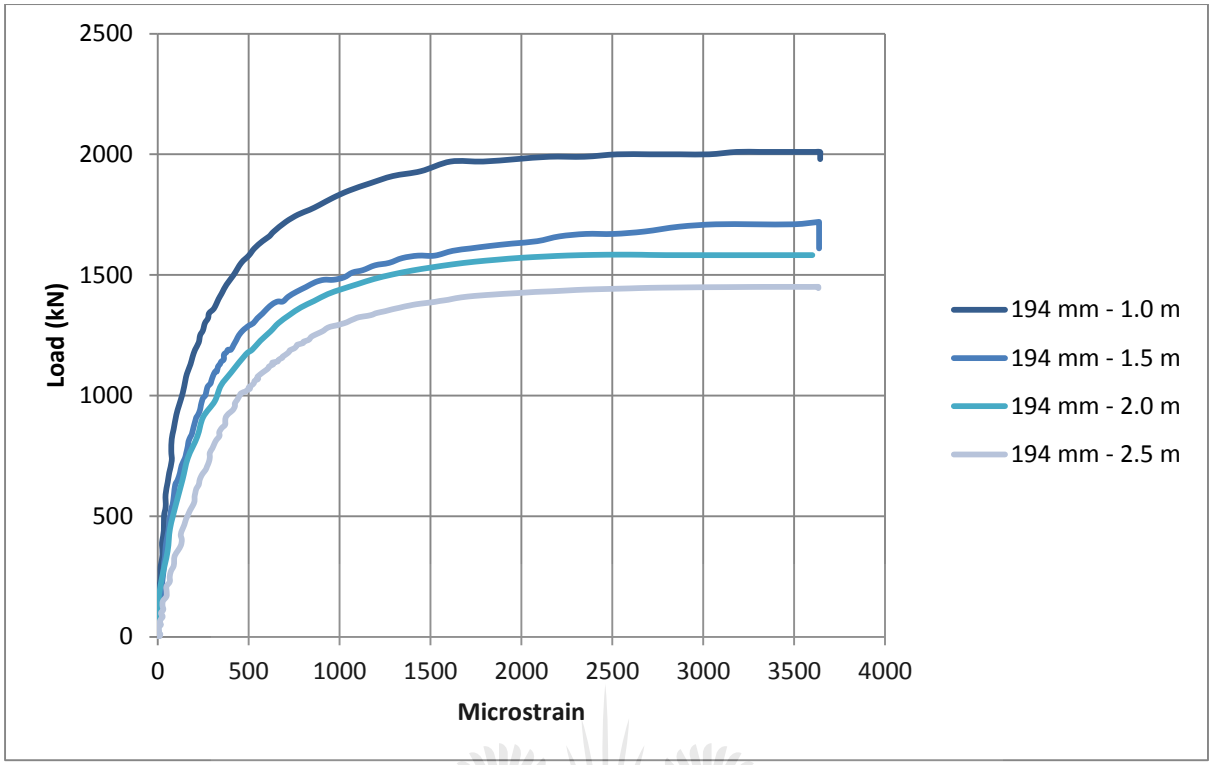

Figure 35 : Comparison of load vs. strain for 194 mm diameter columns

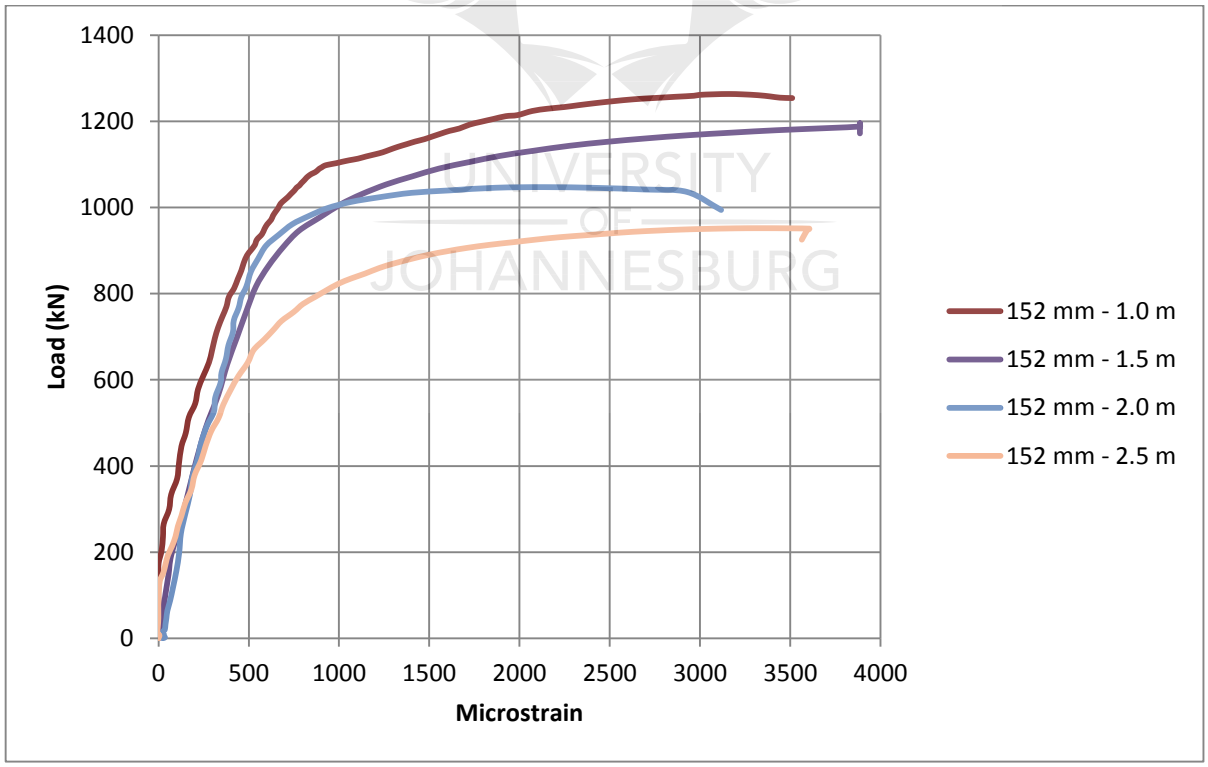

Figure 36 : Comparison of load vs. strain for 152 mm diameter columns

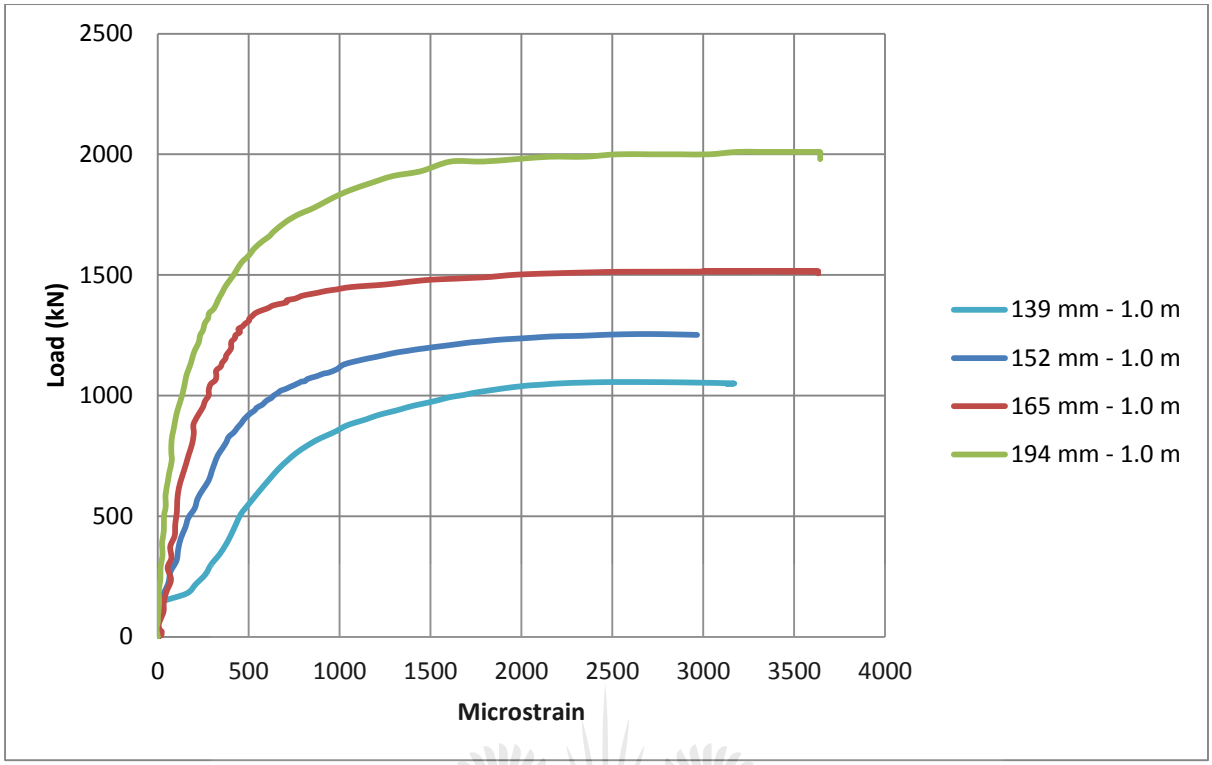

Figure 37 : Comparison of Load vs. strain for 1.0 m length columns

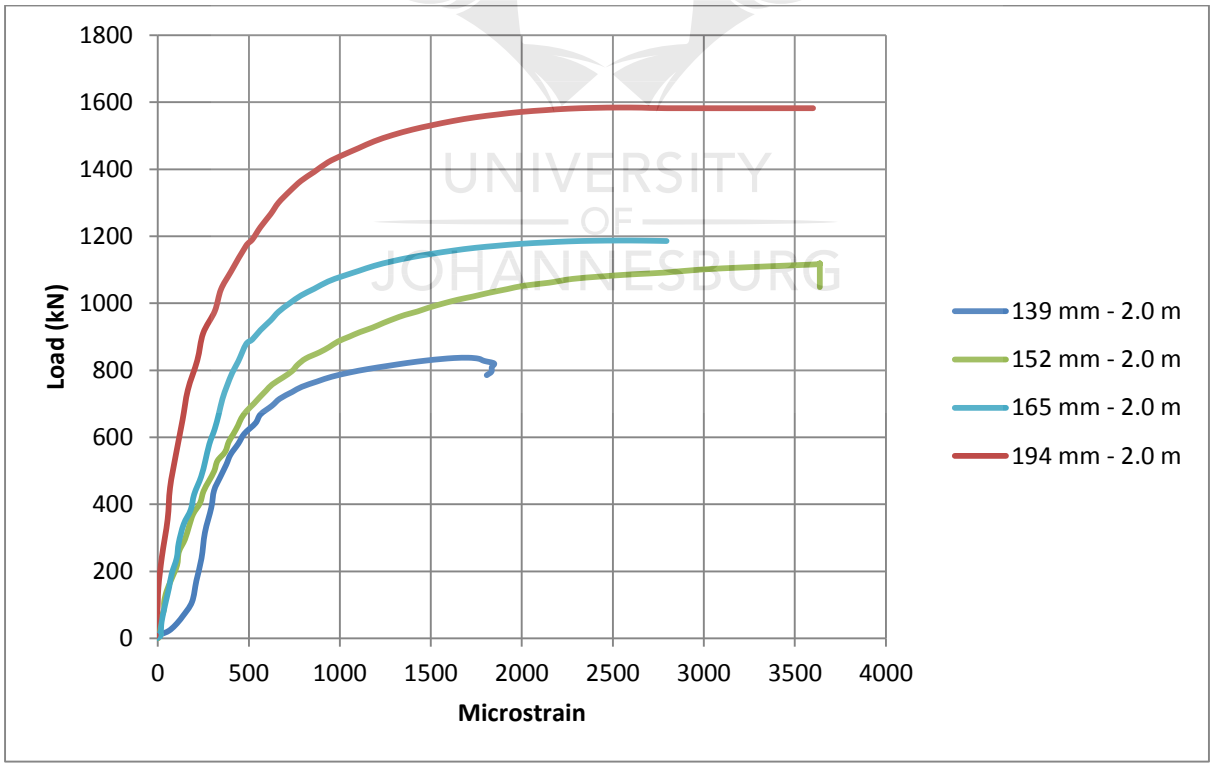

Figure 38 : Comparison of load vs. strain for 2.0 m length columns

4.5 Experimental and predicted ultimate load capacity

4.5.1 Ultimate experimental load capacity of composite columns

The results from the experimental compression test are shown in Table 18. The difference between the average strength of the same samples, for all the tests conducted, is 7.3 kN. This translates into a difference of the average strength of the same samples of 0.4 % when compared to the maximum axial capacity of the columns. A maximum difference of 20 kN was found in Specimens 25 and 26. The reasons for the difference in axial compressive strengths could be a combination of various factors. Factors identified are the small differences in column heights, initial out of straightness of the columns, accurate placement of the columns about their neutral axis while testing, control of the rate of loading and accuracy of levelness of the column surface. If the column lengths differ, this would yield different strengths. Correct placement and out of straightness errors need to be limited as they can cause eccentricities which would give lower axial strengths.

Table 18 : Compression test results

Specimen	Outside diameter (mm)	Length (m)	N_{Test} (kN)	Average (kN)	Difference (kN)	Difference (%)
1	139.7	1.0	1059.2	1057.7	3.1	0.3
2	139.7	1.0	1056.1			
3	139.7	1.5	905.5	903.6	3.9	0.4
4	139.7	1.5	901.6			
5	139.7	2.0	831.7	834.6	5.7	0.7
6	139.7	2.0	837.4			
7	139.7	2.5	732.1	730.6	3.1	0.4
8	139.7	2.5	729.0			
9	152.4	1.0	1263.5	1259.2	8.6	0.7
10	152.4	1.0	1254.9			
11	152.4	1.5	1195.6	1193.4	4.4	0.4
12	152.4	1.5	1191.2			
13	152.4	2.0	1047.3	1044.5	5.7	0.5
14	152.4	2.0	1041.6			
15	152.4	2.5	941.4	945.2	7.6	0.8
16	152.4	2.5	949.0			
17	165.1	1.0	1512.3	1511.5	1.7	0.1
18	165.1	1.0	1510.6			
19	165.1	1.5	1286.4	1280.8	11.3	0.9
20	165.1	1.5	1275.1			
21	165.1	2.0	1187.2	1193.5	12.6	1.1
22	165.1	2.0	1199.8			
23	165.1	2.5	1028.0	1032.3	8.5	0.8
24	165.1	2.5	1036.5			
25	193.7	1.0	2010	2020	20	1.0
26	193.7	1.0	2030			
27	193.7	1.5	1730	1725	10	0.6
28	193.7	1.5	1720			
29	193.7	2.0	1581.6	1582.9	2.5	0.2
30	193.7	2.0	1584.1			
31	193.7	2.5	1451.4	1455.1	7.3	0.5
32	193.7	2.5	1458.7			
				Average Difference	7.3	0.4

4.5.2 Effect of slenderness ratio on ultimate strength

The columns with low slenderness ratios failed by local buckling and crushing of the concrete and the columns with intermediate slenderness ratios failed by a combination of local and overall buckling. The columns with high slenderness ratios failed by overall buckling. Hence, as the slenderness ratio increases the ultimate strength of the columns decreases. The load vs slenderness is plotted in Figure 39

In this research the columns with larger diameters have greater strengths than columns with smaller diameters because the larger diameter columns have a greater area of steel and concrete and the diameter of the inner tube is the same.

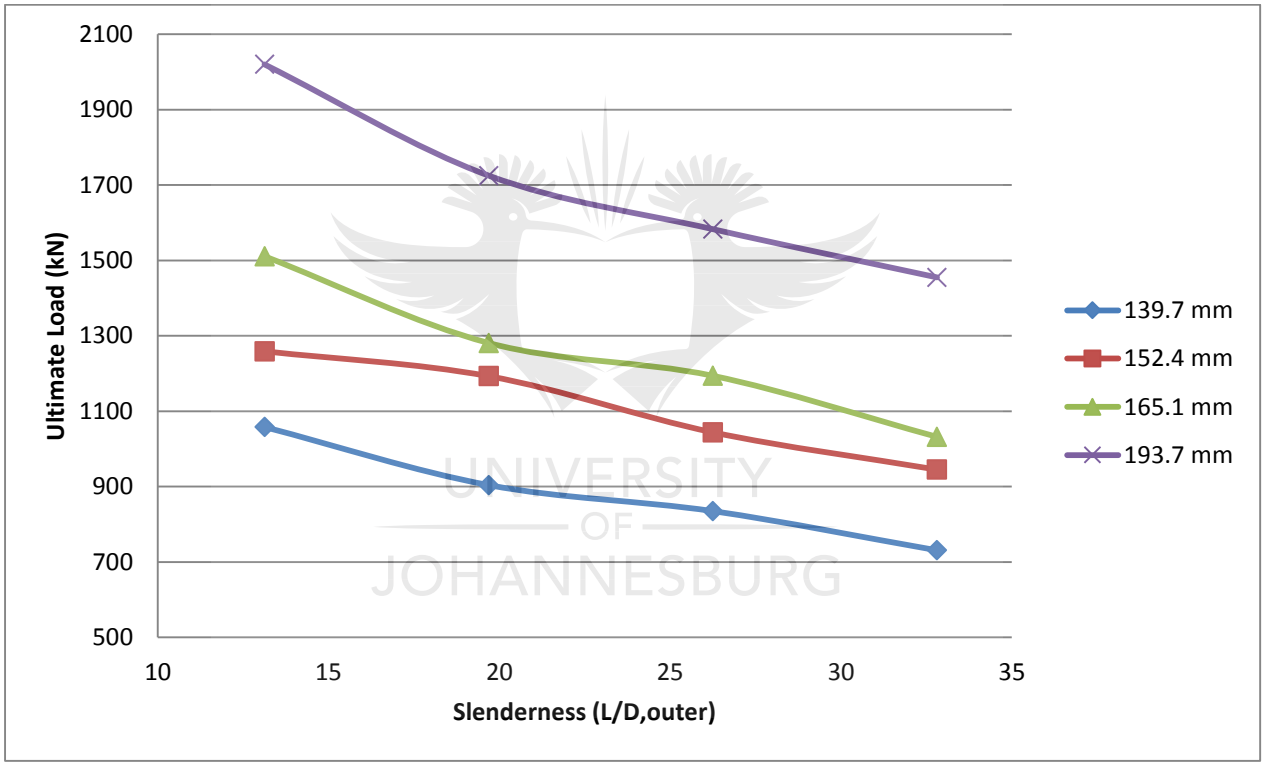

Figure 39: Load vs. slenderness

4.6 Presentation of results in SANS 10162-1 and EC4 formats

4.6.1 Introduction

CFDSCTs are not covered in most design standards of composite columns; however, CFSCTs, which are the closer structural element, are adequately treated in most steel standards (e.g. EC4 and SANS 10162-1). The philosophy employed by EC4 and SANS 10162-1 is to add the individual strengths of the materials and adjust this strength by taking the effect of slenderness into account.

The results found from this experiment are plotted and represented in EC4 and SANS 10162-1 formats. Sections 4.6.2 deals with CFDSCTs written in SANS 10162-1 format and section 4.6.3 deals with CFDSCTs written in EC4 format.

As discussed in chapter 4.5.2, the slenderness ratio has a direct relationship to the ultimate column strength. Hence, it is useful to plot the normalised strength versus the slenderness ratio. Where the dimensionless normalised strength is the experimental compressive strength divided by the sum of the strength of the individual components (two tubes plus the concrete infill). Based on the experimental plots, two best fit curves are proposed for equations to be written in SANS 10162-1 and EC4 format respectively. Both of these curves provide a lower bound design criteria of the test results.

4.6.2 Equations for CFDSCTs written in SANS 10162-1 format

Based on the philosophy that SANS 10162-1 employs, the curve labelled “proposed curve” in Figure 40 was plotted. The curve is based on the formula shown in this subsection. Equations 18 to 25 are based on SANS 10162-1, however, they are adjusted to account for the additional strength that the inner tube provides and the different behaviour between CFDSCTs and CFTs.

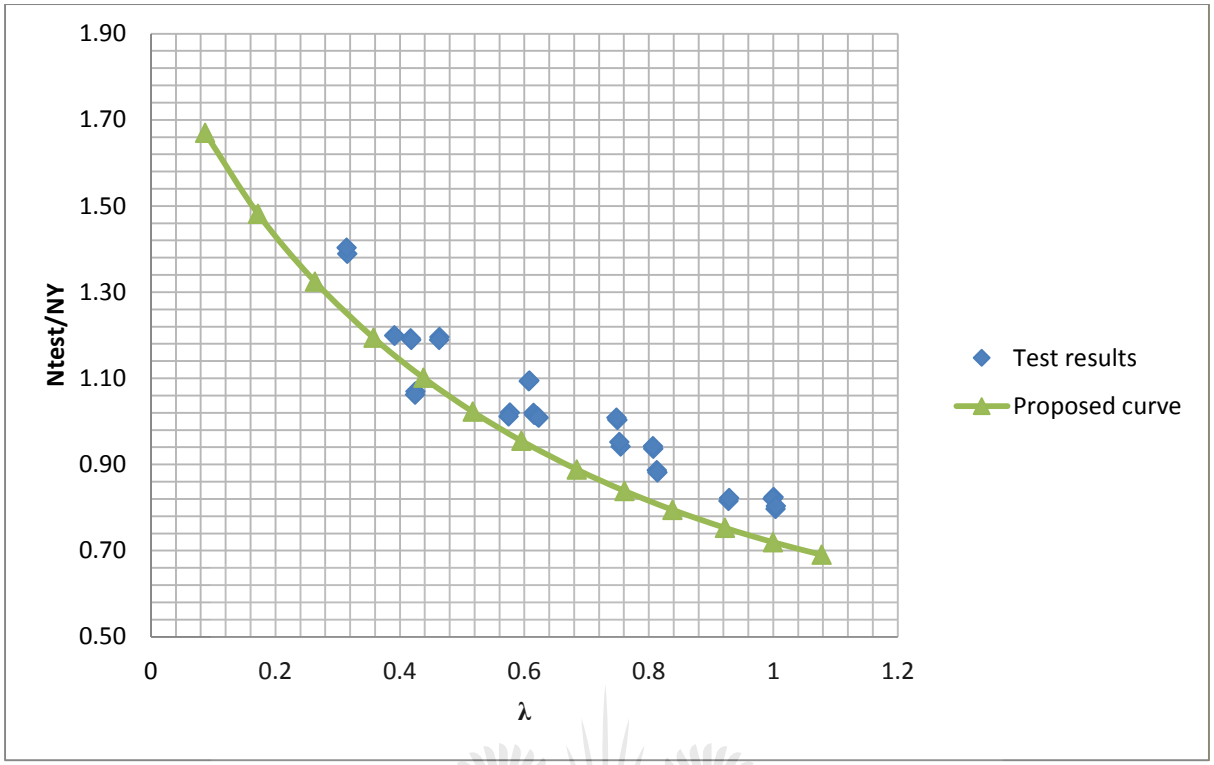

Figure 40: Strength-slenderness ratio relationships (SANS 10162-1)

In Figure 40, N_{Test} is the compressive resistance achieved from the experimental test, N_Y is the yield strength of the column and the slenderness is the non-dimensional slenderness of the CFDSCTs. The compressive resistances are normalised with respect to the yield strength (individual capacity of the two tubes plus the concrete infill).

The results in Figure 40 that have high N_{Test}/N_Y ratios are all stocky columns. This behaviour is because these columns failed by yielding of the steel tubes and crushing of the concrete as compared to the other intermediate to slender columns that failed by overall buckling.

From Figure 40 it can be noted that when the slenderness ratio is above 0.45, the cross-section can be considered to be fully effective. A section can be considered to fully effective when N_{Test}/N_Y is greater than or equal to 1.

Using the experimental values, the best fit curve in Figure 40 is proposed. The curve proved a lower bound design criteria of the test results. From Figure 40, the compressive resistance of the CFDSCTs in axial compression can be predicted by

$$N_p = \tau A_{so} f_{yo} + A_{si} f_{yi} + 0.68\tau' A_c f_{cu} (1 + \lambda^n)^{-1/n} \quad (18)$$

The value of 0.68 is an adjustment factor to correlate the difference in strength between the concrete cube test and the uniaxial concrete strength in the column. The first part of equation 18, $(\tau A_{so} f_{yo})$ represents the outer steel tube strength component, the second part $(A_{si} f_{ysi})$ represents the inner steel tube strength component and $(0.68\tau' A_c f_{cu})$ represents the concrete core strength component and the slenderness of the columns is accounted for by the parameter $(1 + \lambda^n)^{-1/n}$. The value of n is specified as 0.85 and the purpose of this value is to account for the initial out of straightness and residual stresses. This factor is only valid for circular CFDSCTs and not square CFDSCTs because the residual stresses are much lower in a circular tube than a square tube. This is because the residual stresses in a circular tube have a uniform stress distribution.

During the loading process, the concrete infill exerts pressure on the steel tubes in the radial direction. If the slenderness ratio is small then this causes a reduction in the strength of the steel tube.

The steel reduction factor τ_o is calculated from Equation 19;

$$\tau_o = \frac{1.5}{\sqrt{1 + \rho + \rho^2}} \quad (19)$$

$$\text{where} \quad \rho = 0.02\left(25 - \frac{L}{D_o}\right) \quad (20)$$

It can be noted that no reduction is made for the inner tube. This is based on the finding explained in chapter 4.2 that the inner tube did not show signs of local failure.

The reduction in the capacity of the steel tube is due to confinement of concrete. When the concrete is confined, its compressive resistance is increased. The increase in the concrete strength is accounted for using Equation 21;

$$\tau' = 2.5 + \left(\frac{20\rho^2 \tau_o}{D_o/T}\right)\left(\frac{f_y}{0.68 f_{cu}}\right) \quad (21)$$

The relative slenderness is calculated from Equation 22

$$\lambda = \sqrt{\frac{C_p}{C_{ec}}} \tag{22}$$

The slenderness ratio is evaluated as given in Equation 22 and C_p is calculated by equating it to C_{rc} with $\lambda=0$

Parameter $C_{p,}$ is the compressive resistance in Equation 23 and the slenderness (λ) equal to zeroHence;

$$C_p = \tau A_{so} f_{yo} + \tau A_{si} f_{yi} + 0.68\tau' A_c f_{cu} \tag{23}$$

The Euler buckling strength is calculated from Equation 24;

$$C_{ec} = \frac{\pi^2 E I_e}{(KL)^2} \tag{24}$$

The elastic flexural stiffness (EI_e) in equation 24 is obtained by adding the stiffness of the steel and concrete, as given in Equation 25. The stiffness is calculated by multiplying Young's modulus and moment of inertias about the centre for both the steel and concrete

$$EI_e = E_{si} I_{si} + E_{so} I_{so} + 0.6 E_c I_c \tag{25}$$

In the case of this research there is no sustained load. Since the research is a short term experiment, the effects of creep are also not relevant and hence this effect is ignored.

4.6.3 Equations for CFDSCT written in EC4 format

Based on the philosophy that EC4 employs, the curve labelled "proposed curve" in Figure 41 was produced. The curve is based on the formulas shown in this subsection. Equations 26 to 28 are based on EC4, however, they are adjusted to account for the additional strength that the inner tube provides and the different behaviour between CFDSCTs and CFTs.

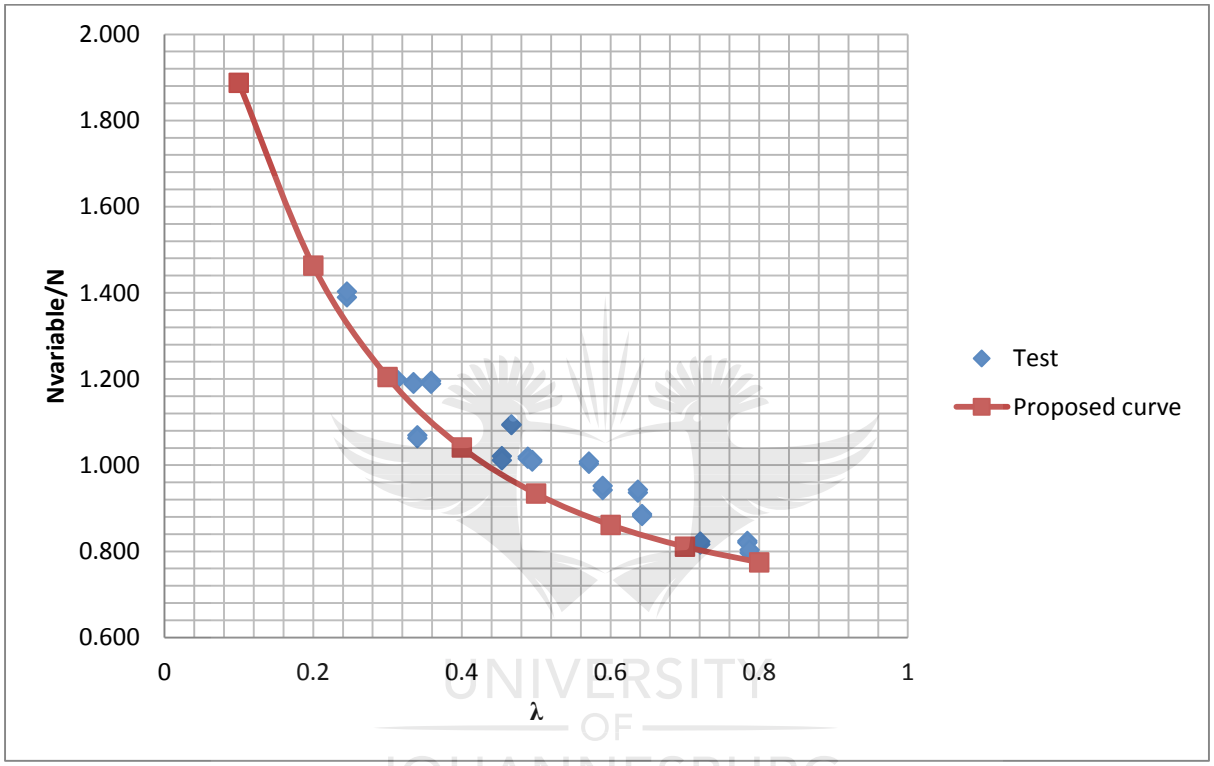

Figure 41 : Strength-slenderness ratio relationships (EC4)

Based on the proposed curve in Figure 41, the final compressive strength of concrete-filled tubes is given by

$$N_p = \chi(A_{so}f_{yo} + A_{si}f_{yi} + A_c f'_{cu}) \quad (26)$$

The value of the reduction factor χ must be less than or equal to one. The reduction factor is calculated from equation 28 or the European strut curves.

$$\chi = 0.65 + \frac{1}{(\phi + \sqrt{\phi^2 - \lambda^2})} \tag{27}$$

Where,

$$\phi = 0.7[1 + \alpha(\lambda - 0.15) + \lambda^2]^2 \tag{28}$$

The imperfection factor for CFSCT column is denoted as α and is equal to 1.9.

4.7 Comparison of test results with proposed equations in SANS 10162-1 format and EC4 format

In sections 4.6.2 to 4.6.3 the proposed curves and equations are discussed. Table 19 shows a comparison of the test strength and the predicted strengths proposed in Equations 18 and 26.

Table 19: Comparison of tests results vs adjusted EC4 and SANS predictions

Hollow section (mm×mm)	Length (m)	N_{Test} (kN)	N_{eq18} (kN)	N_{eq26} (kN)	$\frac{N_{TEST}}{N_{EQ18}}$	$\frac{N_{TEST}}{N_{EQ26}}$
139.7×3	1.0	1058	997	1012	1.06	1.05
139.7×3	1.5	904	835	838	1.08	1.08
139.7×3	2.0	835	721	747	1.16	1.12
139.7×3	2.5	731	639	692	1.14	1.06
152.4×3	1.0	1259	1372	1335	0.92	0.94
152.4×3	1.5	1193	1142	1108	1.04	1.08
152.4×3	2.0	1044	981	990	1.06	1.05
152.4×3	2.5	945	865	920	1.09	1.03
165.1×3	1.0	1511	1557	1489	0.97	1.01
165.1×3	1.5	1281	1306	1232	0.98	1.04
165.1×3	2.0	1194	1127	1094	1.06	1.09
165.1×3	2.5	1032	995	1011	1.04	1.02
193.7×3.5	1.0	2020	2023	1924	1.00	1.05
193.7×3.5	1.5	1725	1733	1591	1.00	1.08
193.7×3.5	2.0	1583	1518	1396	1.04	1.13
193.7×3.5	2.5	1455	1353	1272	1.08	1.14

The average difference between the test results and the code predicted of N_{eq18} and N_{eq26} are 5% and 6%, respectively. Generally, all the test results were found to be very close to the code predicted strengths. The column with a diameter of 165.1mm and a length of 1500 mm has a test to predicted ratio of 0.98. For practical purposes this results can be considered as acceptable. The column with 152.4 mm diameter and a length of 1 m can be regarded as an outlier. These results were then plotted in Figures 42 and 43 to graphically illustrate the difference between the test results versus the SANS 10162-1 and EC4 formats, respectively. Any point above the straight line means that the predicted value is safe. In contrast, points below the line show that the predicted values are high, and hence conservative.

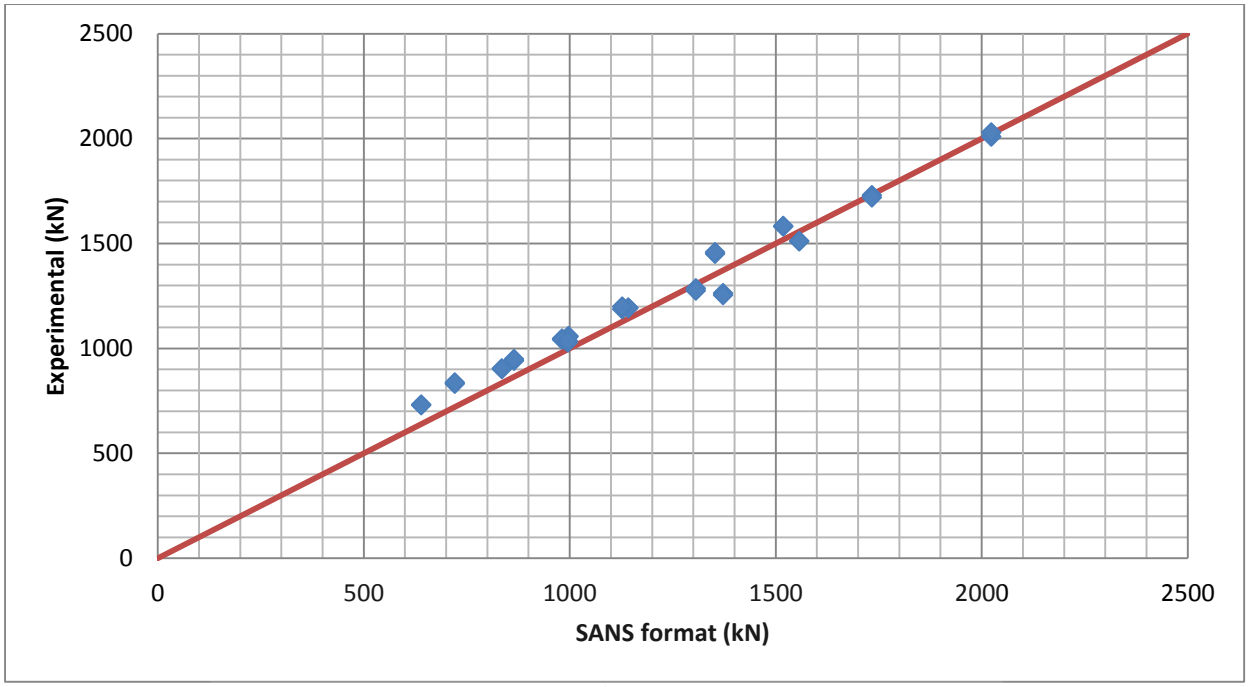

Figure 42: Experimental results vs predicted results in SANS 10162-1 format

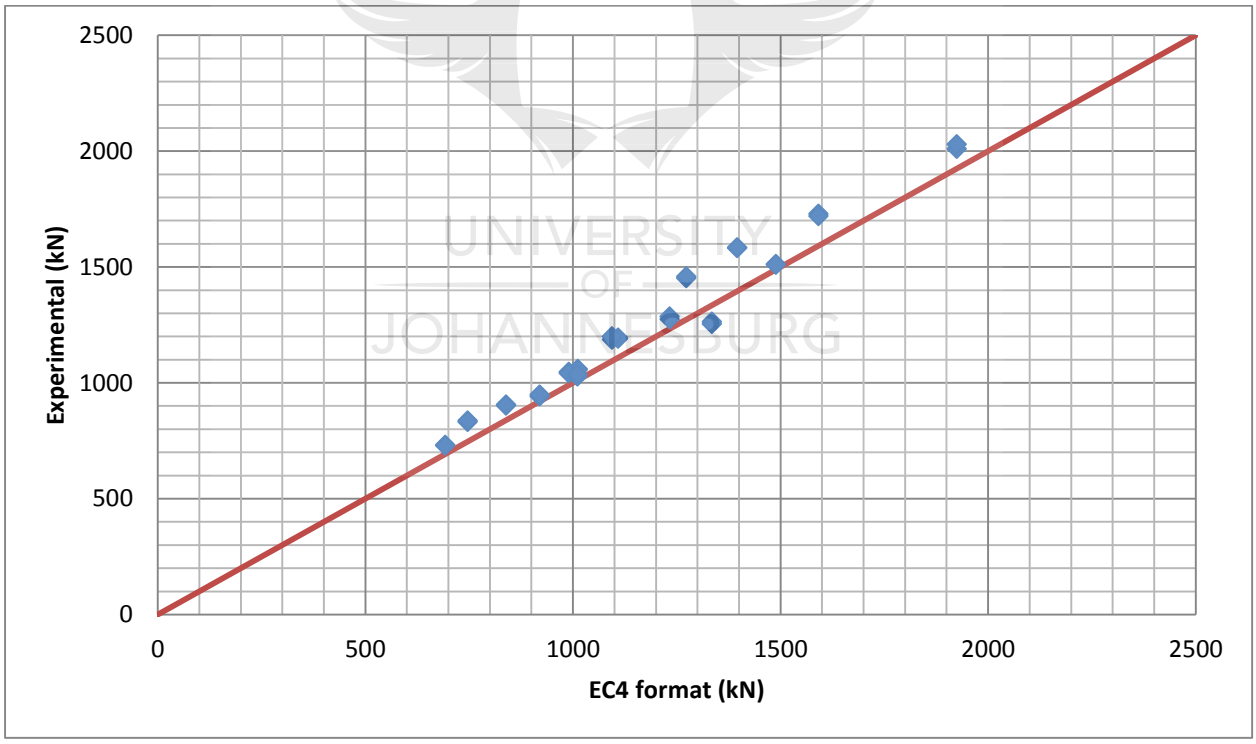

Figure 43 : Experimental results vs predicted results in EC4 format

Figure 42 and 43, graphically illustrates that the experimental results are very close to the predicted results.

5. Summary & Conclusion

The tests conducted on CFDSCTs in current literature only review stub columns. The stub columns are intended to give guidance for the design of long columns. The formulae proposed by the various researchers are reproduced and discussed. Since the formulae's are meant for stub CFDSCTs, they are limited as they do not take the effects of slenderness into account. The lengths of the columns tested by the various authors reviewed varied from 324 to 1050 mm and the outside diameter-to-thickness ratios varied from 19 to 176. The strengths of the concretes and the yield strengths of the steels varied respectively from 216 to 524 MPa and 23 to 78 MPa. It can be noted that while the steel strengths, the concrete strengths and the diameter-to-thickness ratios have been widely varied in the past, the lengths of the columns have not been adequately explored.

The mode of failure of the outer tubes in the literature reviewed was outward local buckling. All authors reviewed also found that the inner tubes of some CSDSCT failed by inward local buckling and shear failure of the concrete infill. This was common in inner tubes with larger diameter-to-thickness ratios.

The availability of concrete confinement varied from author to author. Tao et al's (2004) results suggest that there is no enhancement, Uenaka et al.'s (2010) results suggest that confinement ranges from 0 to 41%, and Wei et al.'s (1995) results suggest that test specimens have an average of 15% confinement. Based on the discussions above it is inconclusive to judge whether there is useful confinement in CFDSCT or not.

The behaviour of 32 CFDSCTs were determined experimentally. The CFDSCTs were concentrically loaded and the compressive strengths were determined at failure. The parameters varied were the outer diameter, outer tube thickness, column length and outer steel tube strength. The column lengths were 1, 1.5, 2 and 2.5 m. The outer steel tube diameters were 139, 152, 165 and 193 mm while the thickness of all the steel tubes was 3 mm, with the exception of the 193 mm diameter tube where the thickness was 3.5 mm. The diameter-to-thickness ratio of the outer tube ranged from 46 to 55. The yield strength of the outer steel tubes varied from 392 to 552 MPa. The inner steel tubes were all from the same batch and the diameter and yield strengths were 76 mm and 324 MPa respectively. The average strength of the concrete cubes was 30.8 MPa. These parameters

were specifically chosen to represent what would commonly be used in engineering practice. Two identical columns were tested with the same set of parameters in order to demonstrate the validity of the test results. The average difference between results for each pair of columns was 0.4 % and hence a good level of confidence can be attributed to the accuracy of the results.

Two types of failures were found from the tests. The 1 m length columns failed by crushing of the concrete core and yielding of the steel tube. This is consistent with the research discussed in the literature review. The 1.5, 2 and 2.5 m columns failed by overall buckling only. This can be attributed to the intermediate to high slenderness ratio of these CFDSCTs columns.

As expected, the compressive capacity of the CFDSCTs decreased when the column lengths were increased. The strengths also increased as the diameters were increased. Since CFDSCTs are not covered in design standards, new formulae were developed to predict their axial compressive capacity. The new formulae are based on the philosophies employed by SANS 10162-1 and EC4 for CFTs. The formulae's are written in a format similar to those for CFTs in SANS10162-1 and EC4. The average differences between the test results and the new formulae are conservatively 5 and 6 %, for SANS10162-1 and EC4, respectively. It can be concluded that both of these formulas can predict the compressive resistance of the CFDSCTs within a close value. Both curves form a lower bound and hence the predicted strengths are safe.

6. Further Research

Most of the research on CFDSCTs focuses on short columns. Short columns are however not representative of engineering practice. Hassanein et al. (2013b) have also identified that more work is required for intermediate to slender columns. To better understand the effects of slenderness of CFDSCT columns more tests should be performed on slender columns.

This research focused on normal strength concrete. The strength of the concrete also needs to be varied to understand the behaviour of low and high strength concrete in CFDSCTs. Though some researchers have used low and high strength concrete, they have not tested intermediate to slender CFDSCTs. Hence, their results do not provide much value for engineering practice.

The results presented in this research can be extended to various degrees of slenderness and other varying properties using a Finite Element program. In this way, the behaviour of slender columns could be better understood.

7. References

BSI (Eurocode 4). (2004). *Design of composite steel and concrete structures, Part 1-1: General rules and rules for buildings*. London: British Standards Institution.

BSI (EN 12390-3). (2009). *Testing hardened concrete - Part 3: Compressive strength of test specimens*. London: British Standards Institution.

Elchalakani, M., Zhao, X-L. & Grzebieta, R. (2002). Test on concrete filled double-skin (CHS outer and SHS inner) composite short columns under axial compression. *Thin-Walled Struct*, 40:415–441.

Hassanein, M.F., Kharoob, O.F. & Liang, Q.Q. (2013). Circular concrete-filled double skin tubular short columns with external stainless steel tubes under axial compression. *Thin-Walled Struct*, 73:252–63.

Hassanein, M.F., Kharoob, O.F. & Liang Q.Q. (2013). Behaviour of circular concrete-filled lean duplex stainless steel tubular short columns. *JThin-Walled Struct*, 68: 113–23.

Han, L-H., Li Y-J. & Liao. F-Y. (2011) Concrete-filled double skin steel tubular(CFDST) columns subjected to long-term sustained loading. *Thin-WalledStruct*, 49:1534–43.

Hibbler, R.C. (2005). Mechanics of materials. Singapore: Prentice Hall

Li, W., Xin Ren Q., Han L-H. & Zhao, X-L. (2012). Behaviour of tapered concrete-filled double skin steel tubular (CFDST) stub columns. *JThin-Walled Struct*, 57:37–48.

Lu, H., Zhao X-L. & Han L-H. (2011) FE modelling and fire resistance design of concrete filled double skin tubular columns. *JConstrSteelRes*, 67:1733–48.

Nakanishi, K., Kitada T. & Nakai H. (1999) Experimental study on ultimate strength and ductility of concrete filled steel columns under strong earthquakes. *JConstrSteelRes*, 51(3):297–319.

SANS (SANS657-1). (2006). *Steel tubes for non-pressure purposes Part 1: Sections for scaffolding, general engineering and structural applications*. Pretoria: Standards South Africa.

SANS (SANS 5860). (2006). *Concrete tests - Dimensions, tolerances and uses of cast test specimens* Pretoria: Standards South Africa.

SANS (SANS 5861-1). (2006). *Concrete tests-Mixing fresh concrete in the laboratory*. Pretoria: Standards South Africa.

SANS (SANS 5861-3:2006). (2006). *Concrete tests, Part 3: Making and curing of test specimens*. Pretoria: Standards South Africa.

SANS (SANS 10100-1). (2000). *The structural use of concrete Part 1: Design*. Pretoria: Standards South Africa.

Tan, K.H. & Zhang, Y.F. (2010). Compressive stiffness and strength of concrete filled double skin (CHS inner & CHS outer) tubes. *JMech Mater Des,* 6:283–291.

Tao, Z., Han, L-H. & Zhao, X-L. (2003). Behaviour of concrete-filled double skin (CHS Inner and CHS Outer) steel tubular stub columns and beam-columns. *JConstr Steel,* 60(8):1129–58.

Uenaka, K., Kitoh, H. & Sonoda, K. (2010). Concrete filled double skin circular stub columns under compression. *Thin-Walled Struct*, 48:19–24.

Wei, S., Mau, S.T., Vipulanandan, C. & Mantrala, S.K. (1995). Performance of new sandwich tube under axial loading: experiment. *JStruct Eng*, 121 (12):1806–14.

Wei, S., Mau, S.T., Vipulanandan, C. & Mantrala, S.K. (1995). Performance of new sandwich tube under axial loading: analysis. *JStruct Eng*, 121(12):1815–21.

Yagishita, F., Kitoh, H., Suimoto, M., Tanihira, T. & Sonoda, K. (2000). Double skin composite tubular columns subjected to cyclic horizontal force and constant axial force. Conference proceedings of the 6th international conference on steel and concrete composite structures held in USA.

Yang, J., Xu, H. & Peng G. (2007). Behaviour of concrete-filled double skin steel tubular columns with octagon section under axial compression. *JChina Civil Engineering Journal*, 40(2): 33–38.

Zhao, X-L. & Grzebieta, R.H. (2002). Strength and ductility of concrete-filled double skin (SHS inner and SHS outer) tubes. *JThin Walled Structures*, 40(2):199-213.

Zhao, X-L., Grzebieta, R. & Elchalakani, M. (2002). Tests of concrete-filled double skin CHS composite stub columns. *JSteel and Composite Structures*, 2:129-146.

Zhao, X-L., & Han, L-H. (2006). Double skin composite construction. *JProg. Struct. Engng Matter*, 8:93-102.

APPENDIX A : SANS 10162-1 CALCULATIONS

D_o	D_i	t_o	t_i	L	A_{so}	A_{si}	L/D_o	D_o/t_o	L/D_i	D_i/t_i	D_i/t_i	I_{so}	I_{si}
mm	mm	mm	mm	mm	mm^2	mm^2						mm^4	mm^4
139.7	76.2	3	2	1000	1288	466	7.2	46.6	13.1	38.1	86.4	3010896	321083
139.7	76.2	3	2	1500	1288	466	10.7	46.6	19.7	38.1	86.4	3010896	321083
139.7	76.2	3	2	2000	1288	466	14.3	46.6	26.2	38.1	86.4	3010896	321083
139.7	76.2	3	2	2500	1288	466	17.9	46.6	32.8	38.1	86.4	3010896	321083
152.4	76.2	3	2	1000	1408	466	6.6	50.8	13.1	38.1	86.4	3930140	321083
152.4	76.2	3	2	1500	1408	466	9.8	50.8	19.7	38.1	86.4	3930140	321083
152.4	76.2	3	2	2000	1408	466	13.1	50.8	26.2	38.1	86.4	3930140	321083
152.4	76.2	3	2	2500	1408	466	16.4	50.8	32.8	38.1	86.4	3930140	321083
165.1	76.2	3	2	1000	1528	466	6.1	55.0	13.1	38.1	86.4	5019713	321083
165.1	76.2	3	2	1500	1528	466	9.1	55.0	19.7	38.1	86.4	5019713	321083
165.1	76.2	3	2	2000	1528	466	12.1	55.0	26.2	38.1	86.4	5019713	321083
165.1	76.2	3	2	2500	1528	466	15.1	55.0	32.8	38.1	86.4	5019713	321083
193.7	76.2	3.5	2	1000	2091	466	5.2	55.3	13.1	38.1	86.4	9460335	321083
193.7	76.2	3.5	2	1500	2091	466	7.7	55.3	19.7	38.1	86.4	9460335	321083
193.7	76.2	3.5	2	2000	2091	466	10.3	55.3	26.2	38.1	86.4	9460335	321083
193.7	76.2	3.5	2	2500	2091	466	12.9	55.3	32.8	38.1	86.4	9460335	321083

E_{so}	E_{si}	f_{yo}	f_{yi}	A_c	I_c	E_c	f_{cu}	ρ_o	τ_o	τ'	C_p	E.Ie	C_{ec}	λ	C_{rc}
MPa	MPa	MPa	MPa	mm^2	mm^4	MPa	MPa				N		N		kN
203233	204958	418	324	9479	14030429	28210	30.8	0.36	1.23	3.84	1577263	9E+11	9E+06	0.42	997
203233	204958	418	324	9479	14030429	28210	30.8	0.29	1.28	3.39	1516067	9E+11	4E+06	0.61	835
203233	204958	418	324	9479	14030429	28210	30.8	0.21	1.34	3.02	1471078	9E+11	2E+06	0.81	721
203233	204958	418	324	9479	14030429	28210	30.8	0.14	1.39	2.74	1444479	9E+11	1E+06	1.00	639
206220	204958	549	324	12273	20894391	28210	30.8	0.37	1.22	4.22	2180047	1E+12	1E+07	0.42	1372
206220	204958	549	324	12273	20894391	28210	30.8	0.30	1.27	3.70	2084996	1E+12	5E+06	0.62	1142
206220	204958	549	324	12273	20894391	28210	30.8	0.24	1.32	3.27	2010390	1E+12	3E+06	0.81	981
206220	204958	549	324	12273	20894391	28210	30.8	0.17	1.37	2.92	1958820	1E+12	2E+06	1.00	865
203530	204958	516	324	15320	29797202	28210	30.8	0.38	1.22	4.06	2412899	2E+12	2E+07	0.39	1557
203530	204958	516	324	15320	29797202	28210	30.8	0.32	1.26	3.64	2312100	2E+12	7E+06	0.58	1306
203530	204958	516	324	15320	29797202	28210	30.8	0.26	1.30	3.28	2229572	2E+12	4E+06	0.75	1127
203530	204958	516	324	15320	29797202	28210	30.8	0.20	1.35	2.97	2167494	2E+12	3E+06	0.93	995
207962	204958	391	324	22816	57986341	28210	30.8	0.40	1.20	3.78	2940208	3E+12	3E+07	0.31	2023
207962	204958	391	324	22816	57986341	28210	30.8	0.35	1.24	3.50	2835378	3E+12	1E+07	0.46	1733
207962	204958	391	324	22816	57986341	28210	30.8	0.29	1.28	3.24	2744630	3E+12	7E+06	0.61	1518
207962	204958	391	324	22816	57986341	28210	30.8	0.24	1.32	3.02	2669426	3E+12	5E+06	0.75	1353

APPENDIX B : EC4 CALCULATIONS

D_o	D_i	t_o	t_i	L	A_{so}	A_{si}	L/D_o	D_o/t_o	L/D_i	D_i/t_i	I_{so}	I_{si}
mm	mm	mm	mm	mm	mm^2	mm^2					mm^4	mm^4
139.7	76.2	3	2	1000	1288	466	7.2	46.6	13.1	38.1	3010896	321083
139.7	76.2	3	2	1500	1288	466	10.7	46.6	19.7	38.1	3010896	321083
139.7	76.2	3	2	2000	1288	466	14.3	46.6	26.2	38.1	3010896	321083
139.7	76.2	3	2	2500	1288	466	17.9	46.6	32.8	38.1	3010896	321083
152.4	76.2	3	2	1000	1408	466	6.6	50.8	13.1	38.1	3930140	321083
152.4	76.2	3	2	1500	1408	466	9.8	50.8	19.7	38.1	3930140	321083
152.4	76.2	3	2	2000	1408	466	13.1	50.8	26.2	38.1	3930140	321083
152.4	76.2	3	2	2500	1408	466	16.4	50.8	32.8	38.1	3930140	321083
165.1	76.2	3	2	1000	1528	466	6.1	55.0	13.1	38.1	5019713	321083
165.1	76.2	3	2	1500	1528	466	9.1	55.0	19.7	38.1	5019713	321083
165.1	76.2	3	2	2000	1528	466	12.1	55.0	26.2	38.1	5019713	321083
165.1	76.2	3	2	2500	1528	466	15.1	55.0	32.8	38.1	5019713	321083
193.7	76.2	3.5	2	1000	2091	466	5.2	55.3	13.1	38.1	9460335	321083
193.7	76.2	3.5	2	1500	2091	466	7.7	55.3	19.7	38.1	9460335	321083
193.7	76.2	3.5	2	2000	2091	466	10.3	55.3	26.2	38.1	9460335	321083
193.7	76.2	3.5	2	2500	2091	466	12.9	55.3	32.8	38.1	9460335	321083

E_{so}	E_{si}	f_{yo}	f_{yi}	A_c	I_c	E_c	f_{cu}	ϕ	χ	α	N	λ	N_p
MPa	MPa	MPa	MPa	mm^2	mm^4	MPa	MPa				kN		kN
203233	204958	418	324	9479	14030429	28210	30.8	1.05	0.49	1.9	888	0.34	1012
203233	204958	418	324	9479	14030429	28210	30.8	1.74	0.29	1.9	888	0.49	838
203233	204958	418	324	9479	14030429	28210	30.8	2.66	0.19	1.9	888	0.64	747
203233	204958	418	324	9479	14030429	28210	30.8	3.90	0.13	1.9	888	0.78	692
206220	204958	549	324	12273	20894391	28210	30.8	1.07	0.48	1.9	1181	0.34	1335
206220	204958	549	324	12273	20894391	28210	30.8	1.77	0.29	1.9	1181	0.49	1108
206220	204958	549	324	12273	20894391	28210	30.8	2.70	0.19	1.9	1181	0.64	990
206220	204958	549	324	12273	20894391	28210	30.8	3.92	0.13	1.9	1181	0.79	920
203530	204958	516	324	15320	29797202	28210	30.8	0.97	0.53	1.9	1260	0.31	1489
203530	204958	516	324	15320	29797202	28210	30.8	1.56	0.33	1.9	1260	0.45	1232
203530	204958	516	324	15320	29797202	28210	30.8	2.33	0.22	1.9	1260	0.59	1094
203530	204958	516	324	15320	29797202	28210	30.8	3.32	0.15	1.9	1260	0.72	1011
207962	204958	391	324	22816	57986341	28210	30.8	0.76	0.68	1.9	1447	0.25	1924
207962	204958	391	324	22816	57986341	28210	30.8	1.14	0.45	1.9	1447	0.36	1591
207962	204958	391	324	22816	57986341	28210	30.8	1.62	0.31	1.9	1447	0.47	1396
207962	204958	391	324	22816	57986341	28210	30.8	2.22	0.23	1.9	1447	0.57	1272